Particle and Fibre Toxicology

RESEARCH

Open Access

Impact of surface functional group modification on cellular internalization and cytotoxicity of silica nanoparticles

Sandra Vranic[1,2,5], Eri Watanabe[1], Kyoka Yamazaki[1], Takatsugu Wakahara[3], Kayoko Miyakawa[1], Sakie Takeuchi[1], Yurika Osada[1], Sahoko Ichihara[4], Wenting Wu[5], Cai Zong[1,5], Toshihiro Sakurai[1], Akira Sato[6], Yasushi Hara[7], Akihiko Ikegami[4], Yuya Terashima[7], Kouji Matsushima[7], Toshihiro Suzuki[7], Ryo Abe[7], Sonja Boland[8], Lang Tran[9] and Gaku Ichihara[1,5*]

Abstract

Background Silica nanoparticles (SiO_2NPs) are widely used in industrial products. Surface modification of SiO_2NPs is one of the promising strategies to develop safer nanomaterials by design. The present study was designed to determine the effects of amino or carboxyl functionalization of rhodamine-labeled SiO_2NPs on cellular uptake and cytotoxicity.

Methods In the in vivo arm of the study, male mice were randomly divided into seven groups (n = 6, each) and exposed to either amino (NH_2)- or carboxyl (COOH)-functionalized, or non-functionalized (OH)-rhodamine-labeled SiO_2NPs at 2 or 10 mg/kg bw, or endotoxin-free water as a control, by pharyngeal aspiration. At 24 h after administration, the mice were euthanized and bronchoalveolar lavage fluid (BALF) was collected for differential cell count and assessment of silica nanoparticle uptake using confocal microscopy. In the in vitro arm of the study, murine RAW264.7 macrophages were exposed to NH_2-or COOH-functionalized or OH- rhodamine-labeled SiO_2NPs. Nonspecific caspase inhibitor, necroptosis inhibitor, pyroptosis inhibitor and autophagy inhibitor were used to determine the roles of cell death signaling in cytotoxicity.

Results The in vivo studies demonstrated significant increase in lung weight at 2 and 10 mg/kg bw by OH-SiO_2NPs but not the other two SiO_2NPs. At 10 mg/kg bw, COOH-SiO2NPs induced a significant increase in BALF macrophages, whereas OH- SiO_2NPs significantly decreased macrophages. OH-SiO_2NPs at 2 mg/kg bw and NH_2- and COOH-SiO_2NPs at 10 mg/kg bw significantly increased BALF neutrophiles. The in vitro studies showed greater NH_2-SiO_2NPs internalization into RAW264.7 macrophages than OH-SiO_2NPs, while OH-SiO_2NPs induced cytotoxicity and upregulation of IL-1β and TNF-α to greater extent than the other two types. Co-treatment with pan-caspase inhibitor and necroptosis inhibitor attenuated (3-(4,5-dimethylthiazol-2-yl)-5-(3-carboxymethoxyphenyl)-2-(4-sulfophenyl)-2H-tetrazolium) (MTS) cytotoxicity of OH-SiO_2NPs.

*Correspondence:
Gaku Ichihara
gak@rs.tus.ac.jp

Full list of author information is available at the end of the article

Conclusion NH_2- or COOH-functionalization reduced the harmful changes observed with OH- SiO_2NPs, which included increase in lung weight and BALF neutrophils at low dose in mice as well as decrease in cell viability and upregulation of proinflammatory cytokines in RAW264.7 macrophages. The results suggested that OH-SiO_2NPs-induced cytotoxicity against macrophages was mediated at least in part through apoptotic/necroptotic signaling but was not related to internalization of particles. The results imply possible development of safer silica nanoparticles by amino- or carboxyl-functionalization of their silanols.

Introduction

Silicon dioxide (silica) nanoparticles (SiO_2NPs) are synthetic amorphous silicon dioxide (SAS) nanoparticles used widely in industrial products as additives for rubber and plastics and as strengthening fillers for concrete. In addition, they are used in the biomedical field for drug delivery and theranostic purposes [1–6].

Silica materials exist in both crystalline and amorphous forms. The most common form of crystalline silica is quartz, whose toxicity has been studied for many years and is linked to chronic bronchitis, emphysema and silicosis [5–7]. Compared to the crystalline micron-sized SiO_2, the amorphous form is known to be less toxic [1, 2]. The toxicological profile of SiO_2NPs has been widely studied recently, with increasing body of literature on the potential adverse effects of SiO_2NP exposure. With regard to the mechanism of toxicity, in vitro studies have shown that the toxic effects of SiO_2NPs are mainly mediated through the induction of oxidative stress and activation of intrinsic or mitochondrial apoptotic pathways [8–13]. Reactive oxygen species (ROS)-mediated cell death is considered one of the main mechanisms of action of many different types of nanomaterials, including SiO_2NPs. However, the results of a recent study indicated that the toxicity of SiO_2NPs is not mediated through intracellular ROS but rather by total silanol content, cell membrane damage, and cell viability [14]. The majority of the in vivo toxicological data are based on acute exposure studies, which usually include intra-tracheal instillation, intravenous injection or oral exposure [1, 2]. Submicron amorphous silica particles were found to have greater inflammatory and cytotoxic potential compared to their bigger counterparts [15]. In the study of Morris et al. [20], C57BL/6 mice were intratracheally instilled with 4 or 20 mg SiO_2NPs /kg body weight. 24 h after instillation, approximately tenfold increase in the cell number was observed in the bronchoalveolar lavage fluid (BALF) of mice treated with the bare SiO2NPs at high dose of 20 mg/kg, compared to the control mice; neutrophils were also increased about 1000- and 500-fold, in BALF of mice treated with the bare SiO_2NPs and amine-functionalized SiO_2NPs at the high dose of 20mg/kg, respectively [16]. Other studies demonstrated acute and chronic exposure to SiO_2NPs aggravated airway inflammation [17–21].

One of the strategies to build "safe by design" NPs is to apply various types of surface modifications to coat the NPs and modulate their internalization into cells or their surface reactivity, thereby decreasing their toxic effects. For example, surface modification of SiO_2NPs was found to reduce their aggregation and nonspecific binding [22], while functionalization with amino or phosphate groups was reported to mitigate their pro-inflammatory and immunomodulatory effects in allergic airway inflammation [17]. Interestingly, coating of SiO_2NPs with polyethylene glycol polymer (PEG) did not efficiently reduce their pro-inflammatory potential in vivo [17, 23]. Furthermore, a few in vitro studies have shown that surface modification of SiO_2NPs reduced their potential for inflammasome activation and cytotoxicity [24, 25].

The present study was designed to determine the effect of surface modification of 30 nm amorphous SiO_2NPs both in vivo (C57BL/6JJcl mice) and in vitro (murine macrophage RAW 264.7 cell line), focusing on the internalization process of these particles into the macrophages, as well as their pro-inflammatory and cytotoxic potentials. Our original hypothesis was that surface modification of amorphous SiO_2NPs should affect their internalization into the macrophages, which is known to be linked to inflammation. However, the results of the in vivo study showed the unexpected results of OH-SiO_2NPs-induced decrease in BALF macrophages. Accordingly, we decided to extend the study to determine the cytotoxicity of OH-SiO_2NPs in vitro and its relation to cell internalization of NPs and gene expression of pro-inflammatory cytokines, as well as the involvement of different cell death pathways in the cytotoxicity. These studies were designed to help understand the mechanism of cytotoxicity induced by non-functionalized OH-SiO_2NPs.

Materials and methods

Silica nanoparticles

Rhodamine-labeled synthetic colloidal amorphous SiO_2NPs, "Sicastar ", of 30 nm in diameter, functionalized with amino group (NH_2-SiO_2NPs, catalog #40-01-301), carboxyl (COOH- SiO_2NPs, catalog #40-02-301) and non-functionalized (OH-SiO_2NPs, catalog #40-00-301) were purchased from Micromod Partikeltechnologie (Rostock, Germany) and used in both the in vitro and in vivo arms of this study.

The NH_2- and COOH-functionalization was introduced by diethylentriamin linker and (triethoxysilyl) propylsuccinic anhydride linker, respectively. The rhodamine-labeled particles were produced by hydrolysis of orthosilicates and compounds with fluorescence. The three types of rhodamine-labeled particles differed only in their surface features but not their crystal structures. All NPs were spherical, nonporous, 2.0 g/cm^3 in density and dispersed in water at 25 mg/mL. The size of the NPs and polydispersity index in water or in complete cell culture medium was characterized by DLS. Zeta-potential was measured with Photal LEZA-600 (Otsuka Denshi Co., Osaka, Japan). The percentages of nitrogen (N), oxygen (O), carbon (C), and silicon (Si) by weight and by atom were measured using scanning electron microscopy (SEM) equipped with energy-dispersive X-ray spectroscopy (EDX) (VE-7800, KEYENCE, Osaka, Japan). The fluorescence intensities of the three types of silica NPs were measured at different concentrations using ARVO^{TM}MX 1420 Multilabel Counter (Perkin Elmer, Waltham, MA). The slopes of the regression lines for the independent variable of concentration and the dependent variable of fluorescence intensity were calculated to obtain the relative fluorescence intensity of the different types of silica NPs labeled with rhodamine.

In vivo studies

Animals

Forty-two male C57BL/6JJcl mice (7 week-old) were purchased from CLEA Japan, Inc. (Tokyo). All mice were housed and acclimatized to the laboratory environment for 1 week in a pathogen-free animal room controlled at 23–25 °C and 55–60% humidity. Light was set within a 12 h light–dark cycle (on at 09:00 and off at 21:00), and food and water were provided ad libitum.

The study was conducted according to the Japanese law on the protection and control of animals and the Animal Experimental Guidelines of Tokyo University of Science. The experimental protocol was approved by the Animal Ethics Committee of Tokyo University of Science (#Y16023).

Mice (mean body weight 22.3 ± 1.1 g, ± SD) were randomly divided into seven groups (n = 6, each) and exposed to either endotoxin-free water (as the control) or NH_2-SiO_2NPs, COOH-SiO_2NPs or OH-SiO_2NPs at 2 or 10 mg/kg bw, which were equivalent to 40 or 200 μg per mouse if body weight was 20 g. These exposure levels were half of those adopted in a previous study, which demonstrated that exposure to SiO_2NPs by intratracheal instillation increased the number of macrophages in BALF at 0.5 mg silica/mouse (20 mg/kg bw) but not at 0.1 mg silica/mouse (4 mg/kg bw) [16]. SiO_2NPs dispersed in water at 25 mg/mL were vortexed and then further diluted with endotoxin-free water to obtain the NP solution at 1 and 5 mg/mL.

Mice were anesthetized with pentobarbital and then exposed to 40 μL aliquot of samples of SiO_2NPs by pharyngeal aspiration, as described previously [26]. The technique of pharyngeal aspiration involved placement of the NPs suspension on the back of the tongue followed by pulling of the tongue to induce a reflex gasp with resultant aspiration of the droplets. At 24 h after administration, the mice were euthanized by intraperitoneal injection of pentobarbital. Bronchoalveolar lavage (BAL) was performed by cannulation of the trachea with 18-gauge needle, and infusion and collection of 5/6 mL of saline was repeated six times. The 24 h post-administration time point was selected to observe early inflammatory responses.

BALF total and differential cell counts

The recovered bronchoalveolar lavage fluid (BALF) was centrifuged (1,500 rpm, 5 min, 4°C), and the cell pellet was mixed with 1 mL of ACK lysing buffer (Gibco-Thermo Fischer Scientific, Waltham, MA) for hemolysis. Next, 10 mL of Dulbecco's phosphate buffer saline (DPBS) was added before centrifugation at 1500 rpm and 4 °C. The resultant pellet was re-suspended in DPBS for total and differential cell counts. BALF total cell count was measured using hematocell counter. Aliquots of 5×10^4 cells in 400 μl DPBS per slide were prepared for cytospins. The cell mixture was added to EZ Single Cytofunnel®, Thermo, UK and centrifuged for 10 min at 1000 rpm with Cytospin, using cytoslides. The slides were dried overnight at room temperature and then stained with the Differential Quik Stain Kit (Modified Giemsa, Sysmex Co., Kobe, Japan) for differential cell count in 10 fields on each slide (20 ×magnification).

Fluorescence immunocytology

The slides obtained by Cytospin were washed three times in DPBS and then incubated with blocking agent (1% BSA) for one hour. The slides were further incubated with Biotin anti-Ly6G and Ly6C (Gr-1) (BD, Franklin Lakes, NJ), which was diluted 400 folds in 1% BSA, for one hour at room temperature, washed in DPBS three times and then incubated with 200-fold diluted Cy5 streptavidin (BioLegend, San Diego, CA) for 30 min at room temperature to stain the neutrophils. Ly6G and Ly6C (Gr-1) were used as markers of neutrophils, as their expression levels are known to correlate with differentiation and maturation of granulocytes [27, 28] and are only expressed transiently on bone marrow cells in the monocyte lineage [28]. The slides were counterstained with Hochest33342 for 10 min at room temperature and enclosed with Fluorescent Mounting Media (Dako, Agilent, Santa Clara,

CA). Cells and SiO_2NPs were observed with a confocal microscope (model Fv10i, Olympus, Tokyo).

In vitro studies

Cell culture

Murine macrophages RAW 264.7 cell were kindly provided by Prof. Kenneth Dawson, University of College Dublin and grown in Dulbecco's Modified Eagle Medium (DMEM, high glucose) with L-glutamine and phenol red (Wako, catalog #044-29765) supplemented with 1 mM sodium pyruvate (100 mM, Gibco, catalog #11,360–070), 100 U/mL penicillin, 100 mg/mL streptomycin and 250 ng/mL amphotericin B (anti-anti, Gibco, catalog #15,240-062), 2 mM glutamine and 10% FBS. All experiments were performed with cells from passages 4 to 15. Cells were grown in T25-flasks (Violamo, AS ONE Co., Osaka) in monolayers. Exponentially growing cells were maintained under a humidified atmosphere of 5% CO_2 and 95% air at 37 °C and were passaged once every two days using a cell scraper (NEST 100071).

NP treatment

Depending on the experiment and after reaching 70–80% confluence, the RAW 264.7 cells were seeded onto appropriate cell culture plates and treated with one of the three SiO_2NPs. Before exposure to SiO_2NPs, the RAW 264.7 cells were rinsed with PBS to eliminate trace amounts of FBS. Treatments were performed under FBS-free condition for three reasons: (1) serum is reported to modulate NPs uptake [29], and (2) to mimic in vivo condition whereby bronchial cells are not directly exposed to serum proteins. (3) bovine serum albumin (BSA) is known to induce agglomeration of SiO_2NPs [30]. Stock of 30 nm rhodamine-labeled silica nanoparticles (25 mg/mL in water) was vortexed shortly before the preparation of the final dilution for the treatment.

MTS assay

The (3-(4,5-dimethylthiazol-2-yl)-5-(3-carboxymethoxyphenyl)-2-(4-sulfophenyl)-2H-tetrazolium) (MTS) assay was conducted using CellTiter 96® Aqueous One Solution Cell Proliferation Assay (Promega, Madison, WI), as described previously [31] using the instructions provided by the manufacturer. Briefly, RAW264.7 cells were seeded at 1.5×10^4 cells/well onto 96-well plates and incubated at 37 °C under a humidified atmosphere of 5% CO_2 and 95% air for 24 h. After incubation, the cell culture medium was removed from each well with a multichannel pipette, and the cells were washed three times with DPBS to remove FBS. The cells were incubated for 4 or 24 h with one of the three types of SiO_2NPs dispersed in FBS-free cell culture medium at a final concentration ranging from 0.3 to 30 μg/cm^2. After incubation with the SiO_2NPs, the cells were washed twice with DPBS, and incubated with MTS reagent (1.4 mL CellTiter 96® AQueous One Solution Reagent and 7.1 mL of complete phenol red-free cell culture medium with FBS). Cell viability was determined by measuring absorbance at 490 nm, which reflected the reduction of {3-(4,5-dimethylthiazol-2-yl)-5-(3-carboxymethoxyphenyl)-2-(4-sulfophenyl)-2H-tetrazolium} (MTS) to formazan by mitochondria in viable cells.

Evaluation of OH-SiO_2NPs-induced interference in MTS assay

Possible interference by hydroxylated silica nanoparticles (OH-SiO_2NPs) in the MTS assay was evaluated following the method of Hirsch [32]. OH-SiO_2NPs were dispersed in fetal bovine serum (FBS)-free cell culture medium at final concentrations ranging from 0.3 to 30 μg/cm^2 and incubated for 60 min at 37 °C in 5% CO_2 with one of the following: (1) phenol red-free cell culture medium; (2) phenol red-free medium mixed with CellTiter 96® AQueous One Solution Reagent at a 5:1 ratio; or (3) 5 mL of phenol red-free medium containing 1 mL of CellTiter 96® AQueous One Solution Reagent and 50 μL of Na_2SO_3. After incubation, absorbance was measured at 490 nm.

Confocal microscopy

RAW 264.7 cells were seeded in 8 well Lab-TekII™ chambered cover glasses (Nunc, Thermo Scientific, Dominique Dutscher, Brumath, France) at 16,590 cells/well in complete cell culture medium, and then incubated for 24 h. Upon 70–80% confluence, the cells were washed three times with DPBS to remove FBS and treated with 0.3 mL/well of NPs at pre-selected concentrations for 24 h at 37 °C and 5% CO_2. After removal of the medium, the cells were washed once and fixed in 4% paraformaldehyde for 20 min at 25 °C, rinsed twice with DPBS and then incubated with Cell Mask Green Plasma Membrane Stain (C37608 Thermo Fisher Science, Waltham, MA) and Hoechst for 10 min. The cells were washed with DPBS twice. After embedding the cells in Mounting Medium, they were observed by confocal microscopy (model FV.10, Olympus, Tokyo). The maximum concentration of silica NPs of 35.2×10^5 μg/cell (8.37 μg/cm^2) was determined to be equivalent to exposure level of 40 μg/mouse in vivo, given that the average number of macrophages collected in BALF was 1.14×10^5 cells/mouse.

Flow cytometry

RAW264.7 cells were seeded onto 6-well plates at 2.37×10^4 cells/cm^2 in complete cell culture medium and incubated for 24 h before treatment. After treatment with 3.0 mL/well of SiO_2NPs at preselected concentrations for 1 or 4 h in dark, the medium was removed, cultures were thoroughly washed with PBS three times and treated with 0.1% trypan blue for 1 min to quench the fluorescence of

rhodamine on the cell surface. The concentration of trypan blue for quenching the fluorescence of rhodamine was determined beforehand by plotting trypan blue and rhodamine intensity in RAW264.7 cells exposed to OH-rhodamine-labeled SiO_2NPs. The cells were washed with PBS, mixed with 500 µL of FACS buffer (PBS containing 0.5% FBS and 0.1% NaN_3) and harvested by cell scraper. Cell-associated fluorescence was detected using FACS-Calibur™ and results were analyzed with FlowJo software (BD, Franklin Lakes, NJ). The mean fluorescence intensity (MFI) of rhodamine (excitation 488 nm, Filter range 564–606 nm) from three different size fractions indicated by the forward scatter (FS) was computed by the flow cytometer. The results are reported as the median of the distribution of cell fluorescence intensity obtained by analyzing cells in the gate. To adjust for the differences in the fluorescence intensity relative to weight, the intensity of rhodamine fluorescence was measured at different concentrations of three types of S SiO_2NPs using ARVOMx-fla system (485 nm/535 nm 1.0 s).

LDH cytotoxicity assay

The LDH cytotoxicity assay was conducted to quantify cytotoxicity by measuring the release of the enzyme lactate dehydrogenase (LDH) from damaged cells into the culture medium. The assay was conducted using Pierce LDH cytotoxicity assay kit following the instructions provided by the manufacturer (Thermo Fisher Scientific, Waltham, MA). Briefly, RAW264.1 cells were plated at 10^4 cells/well in 100 µl of medium in a 96-well tissue culture plate. After incubation at 37 C under 5% CO_2 for 24 h, the cells were exposed to NH_2-, COOH-functionalized, OH-rhodamine-labeled non-functionalized SiO_2NPs at 5.85 µg/cm^2 (19.5 µg/mL). After exposure for 1, 4, 12, 24, 36 and 48 h, the supernatant of the culture medium was collected by centrifugation, and dispensed at 50 µl/well into another 96-well plate. Each cell was incubated in the presence of 50 µl of LDH reaction mixture at room temperature for 30 min under darkness. The reaction was stopped by adding 50 µl of stop solution, and absorbance at 490 and 680 nm was read by Plate reader Gen5 (BioBik, Osaka).

Evaluation of cell death by cell proliferation assay

Cell death pathways involved in the cytotoxicity of OH-SiO_2NPs were examined using the following inhibitors: cell-permeable pan-caspase inhibitor Z-VAD-FMK (#G7231A, Promega, Madison, WI, USA), necroptosis inhibitors (RIP1-specific inhibitors) necrostatin-1, (#11,658, Cayman Chemical, Ann Arbor, MI, USA) and GSK"963 (#S864201, Sellekchem, Houston, TX, USA), pyroptosis inhibitor (caspase-1 and -4 inhibitor) Z-YVAD-FMK (#ab141388, Abcam, Cambridge, UK) and autophagy inhibitor (inhibitor of autophagosome-lysosome fusion) chloroquine diphosphate salt (#C-6628, Sigma-Aldrich, Saint Louis, MO, USA). Z-VAD-FMK, necrostatin-1, GSK'963 and Z-YVAD-FMK were each dissolved at 20 or 50 mM in dimethyl sulfoxide (DMSO), and chloroquine diphosphate salt was dissolved at 40 mM in endotoxin-free water. Each of the resultant inhibitor in vehicle was further diluted by the culture medium to the final concentration. RAW264.1 cells were preincubated with Z-VAD-FMK, necrostatin-1, Z-YVAD-FMK or chloroquine, or co-treated with Z-VAD-FMK and GSK'963, or corresponding vehicle for 1 h, and exposed to plain rhodamine-labeled silica NPs at 28 µg/mL for 18 h. The cytotoxicity assay was conducted for each inhibitor to determine the maximum concentration of the inhibitor associated with lack of decrease in cell viability. Cytotoxicity was evaluated using CellTiter 96® Aqueous One Solution Cell Proliferation Assay (Promega) as mentioned above.

Nuclear staining by DAPI

RAW264.1 cells were plated at a density of 1.5×10^4 cells per well in 200 µL of medium in a 96-well tissue culture plate. After incubation at 37 °C under 5% CO_2 for 24 h, the cells were exposed to OH–rhodamine-labeled non-functionalized SiO_2NPs at a concentration of 28 µg/cm^2. Following an 18 h exposure, the culture medium was removed, and the cells were washed once with D-PBS, then fixed with 4% paraformaldehyde (PFA) for 10 min. After removal of the fixative, the cells were washed three times with DPBS, stained with 4',6-diamidino-2-phenylindole (DAPI)for 1 min, and mounted using mounting medium (#ab104135, Abcam, Cambridge, UK). The cells were observed under a fluorescence microscope (DMI6000 B, Leica, Wetzlar, Germany) equipped with a digital camera (DFC365 FX, Leica, Wetzlar, Germany).

Quantitative real-time PCR

Quantitative RT-PCR was used to quantify the mRNA levels of various pro-inflammatory cytokines induced by SiO_2NPs. For this purpose, RAW264.1 cells were seeded onto 6-well plates at 23,700 cells/cm^2 and exposed to silica NPs at concentrations of 0.33, 1.67 and 8.37 µg/cm^2 (1.06, 5.30, and 26.50 µg/mL, respectively). The cells were collected by centrifugation at 1000 rpm for 5 min at 4 °C. Total RNA from the cells was isolated by using ReliaPrep™ RNA Cell Miniprep System (Promega, Fitchburg, WI). The concentration of total RNA was quantified by spectrophotometry (ND-1000; NanoDrop Technologies, Wilmington, DE). RNA was reverse transcribed to single-strand cDNA using SuperScript III First-Strand Synthesis System for RT-PCXR (Life Technologies). The cDNA was subjected to quantitative real-time PCR (qRT-PCR) analysis with Thunderbird cyber green master mix

(TOYOBO, Osaka) and primers designed by TAKARA (Kusatsu, Japan). The primers were.

5′—GTCCCTCAACGGAAGAACCAA—3′ (forward) and 5′—TCTCAGACAGCGAGGCACAT—3′ (reverse) for MIP-2, 5′-

5'- CATCCACGTGTTGGCTCA (forward) and 5'- GA TCATCTTGCTGGTGAATGAGT-3' (reverse) for MCP-1, 5'-AGCTTCAGGCAGGCAGTATC-3' (forward) and 5'-GTCACAGAGGATGGGCTCTT-3' (reverse) for IL-1β,

5'-GATCGGTCCCCAAAGGGATG-3' (forward) and 5'-GTGGTTTGTGAGTGTGAGGGT-3' (reverse) for TNF-α,

and 5'-GATCATTGCTCCTCCTGAGC-3' (forward) and 5'-ACTCCTGCTTGCTGATCCA-3' (reverse) for β-actin. 5'-GCCTGGAGAAACCTGCCAA-3' (forward) and 5'-TGAAGTCGCAGGAGACAACC-3' (reverse) for GAPDH, 5'-GTTCCAGCACATTTTGCGAGT-3' (forward) and 5'- GGTGAGGTCGATGTCTGCTT-3' (reverse) for 18S ribosomal RNA,

A standard curve was constructed by serial dilutions of the cDNA sample. All PCR reactions were performed in duplicates and the values were expressed relative to the geometric mean of β-actin mRNA, GAPDH mRNA, and 18S r RNA level. The average of the two reactions was used as the representative mRNA value for each mouse.

Statistical analysis

Data are expressed as mean ± standard deviation (SD). Differences between the test samples and control or among the groups were analyzed respectively by one-way ANOVA followed by Dunnett or Tukey multiple comparison test. Multiple regression analysis with dummy variables for the different types of particles was conducted to test the interaction between SiO_2NP level and the type of NPs. Dummy variable $[NH_2] = 1$, when the type was NH_2-SiO_2NPs; $[NH_2] = -1$, when the type was OH- SiO_2NPs; and $[NH_2] = 0$, otherwise. Dummy variable [COOH] = 1, when the type was COOH- SiO_2NPs; [COOH] = − 1, when the type was OH-SiO_2NPs; and [COOH] = 0, otherwise. Statistical significance was set at 5%. For the analysis of relative fluorescence intensity among different types of NPs, regression lines were obtained by forcing the intercept to zero using Excel 2016 (Microsoft, Redmond, WA). All statistical analyses were performed using JMP (version 14, SAS Institute, Cary, NC).

Results

Larger hydrodynamic diameter of OH-SiO_2NPs relative to NH_2 and COOH-SiO_2NPs

To understand the physicochemical features of the three types of SiO_2NPs, the hydrodynamic diameters and zeta potentials were determined by DLS and Zeta potential measurements, both in water (since the materials were dispersed in endotoxin-free, ultra-pure water for pharyngeal aspiration in mice) and in the cell culture medium (relevant to the exposure of RAW264.8 cells). The mean hydrodynamic diameter of the OH-SiO_2NPs was significantly larger than those of the NH_2- and COOH-SiO_2NPs in water and in FBS-free cell culture medium (Table 1). On the other hand, polydispersity index was significantly greater in COOH-SiO_2NPs than OH-SiO_2NPs but was less than 0.7 both in water and FBS-free cell culture medium, indicating appropriate condition for DLS measurement. The physicochemical features of the three types of SiO_2NPs (in water and in FBS-free cell culture medium) had no effect on the Zeta potential. The pH of OH- SiO_2NPs was significantly lower than that of NH_2- SiO_2NPs in water while there was no significant difference in the pH among the three types of SiO_2NPs in FBS-free cell culture medium.

OH-SiO_2NPs, NH_2-SiO_2NPs and COOH-SiO_2NPs showed relatively higher abundance of O, N and Si element, respectively, compared with the other types of SiO_2NPs

SEM-DEX analysis revealed that the surface of NH_2-SiO_2NPs contained significantly higher amounts of nitrogen (N) and carbon (C), both by weight and by atom, than that of OH-SiO_2NPs (Table 2). In contrast, OH-SiO_2NPs exhibited significantly higher oxygen (O) content, both by weight and by atom, than the other types of SiO_2NPs. The surface of COOH-SiO_2NPs contained significantly more silicon (Si), both by weight and by atom,

Table 1 Physicochemical properties of SiO_2NPs dispersed in water and in complete cell culture medium, studied by DLS and Zeta potential measurement

Type of SiO2NPs	Solvent	Hydrodynamic diameter (nm)	Polydispersity index	Zeta potential (mV)	pH
NH_2-SiO_2NPs	Water	30.91 ± 0.02§	0.12 ± 0.02§¶	− 21.0 ± 6.2§	6.51 ± 0.12§
COOH-SiO_2NPs	Water	29.25 ± 0.48§	0.15 ± 0.04§	− 29.4 ± 7.3§	6.26 ± 0.27§¶
OH- SiO_2NPs	Water	33.87 ± 1.11¶	0.12 ± 0.02¶	− 22.3 ± 2.7§	5.92 ± 0.10¶
NH_2-SiO_2NPs	FBS-free medium	31.68 ± 0.40§	0.19 ± 0.01§¶	− 20.0 ± 0.8§	7.97 ± 0.12§
COOH-SiO_2NPs	FBS-free medium	29.36 ± 0.28¶	0.25 ± 0.08§	− 19.8 ± 1.4§	7.94 ± 0.12§
OH- SiO_2NPs	FBS-free medium	34.87 ± 0.38†	0.17 ± 0.03¶	− 16.1 ± 2.9§	7.93 ± 0.17§

Data are mean ± SD of three measurements. Tukey–Kramer multiple comparison was conducted following ANOVA between NH_2-SiO_2NPs, COOH-SiO_2NPs and OH-SiO_2NPs in each of Water or FBS-free medium. There is a significant difference between the different types of SiO_2NPs, which are not marked by the same symbols. Significance level was set at 5%

Table 2 Element ratio of SiO_2NPs quantified by SEM–EDX

			Percentage	
Element	**Type of SiO_2NPs**	**N**	**By weight**	**By atom**
N	NH_2-SiO_2NPs	3	4.24 ± 0.25*	5.55 ± 0.31*
	COOH-SiO_2NPs	3	3.61 ± 0.04	4.85 ± 0.05
	OH-SiO_2NPs	3	3.18 ± 0.39	4.24 ± 0.50
O	NH_2-SiO_2NPs	3	40.7 ± 0.2*	46.6 ± 0.2*
	COOH-SiO_2NPs	3	41.9 ± 0.3*	49.3 ± 0.4*
	OH-SiO_2NPs	3	44.7 ± 0.4	52.2 ± 0.7
C	NH_2-SiO_2NPs	3	13.8 ± 0.2*	21.0 ± 0.2*
	COOH-SiO_2NPs	3	10.3 ± 0.3	16.2 ± 0.5
	OH-SiO_2NPs	3	10.0 ± 0.5	15.6 ± 0.7
Si	NH_2-SiO_2NPs	3	41.3 ± 0.3*	26.9 ± 0.3*
	COOH-SiO_2NPs	3	44.2 ± 0.1*	29.6 ± 0.1*
	OH-SiO_2NPs	3	42.1 ± 0.5	28.0 ± 0.5

*P < 0.05, compared to OH-SiO_2NPs by ANOVA followed by Dunnett's multiple comparison. SEM–EDX: scanning electron microscopy equipped with energy-dispersive X-ray spectroscopy

Table 3 Weight of body and lungs of mice at 24 h after exposure to SiO_2NP by pharyngeal aspiration

	Concentration of SiO_2NPs (mg/kg bw)	**n**	**Body weight (g)**	**Lung weight (mg)**
Vehicle	0	6	20.9 ± 1.4	293 ± 22
NH_2-SiO_2NPs				
	2	6	21.6 ± 0.4	301 ± 5
	10	6	21.3 ± 1.4	321 ± 23
COOH-SiO_2NPs				
	2	6	21.6 ± 1.2	305 ± 16
	10	6	21.5 ± 1.0	322 ± 6
OH-SiO_2NPs				
	2	6	21 ± 1	324 ± 25*
	10	6	20 ± 1	331 ± 16*

*P < 0.05, compared to the vehicle control, by ANOVA followed by Dunnett's multiple comparison. Multiple regression analysis with dummy variables for types of particles did not show any significant interaction for body and lung weights

whereas NH_2-SiO_2NPs had significantly less Si compared with OH-SiO_2NPs.

In vivo experiments

OH-SiO_2NPs increased lung weight in vivo

To evaluate the effects of each functional group on the toxicity of the three types of SiO_2NPs, we measured body and lung weights in mice exposed to each type of SiO_2NPs. Pharyngeal aspiration of these SiO_2NPs at 2 or 10 m/kg bw had no effect on body weight (Table 3). On the other hand, the non-functional OH- SiO_2NPs, but not NH_2- or COOH- SiO_2NPs, induced a significant increase in lung weight at both 2 and 10 mg/kg bw. These results suggest that OH- SiO_2NP is injurious to the lung of mice, causing increased lung weight in vivo and that NH_2- and COOH-functionalization mitigated this harmful effect.

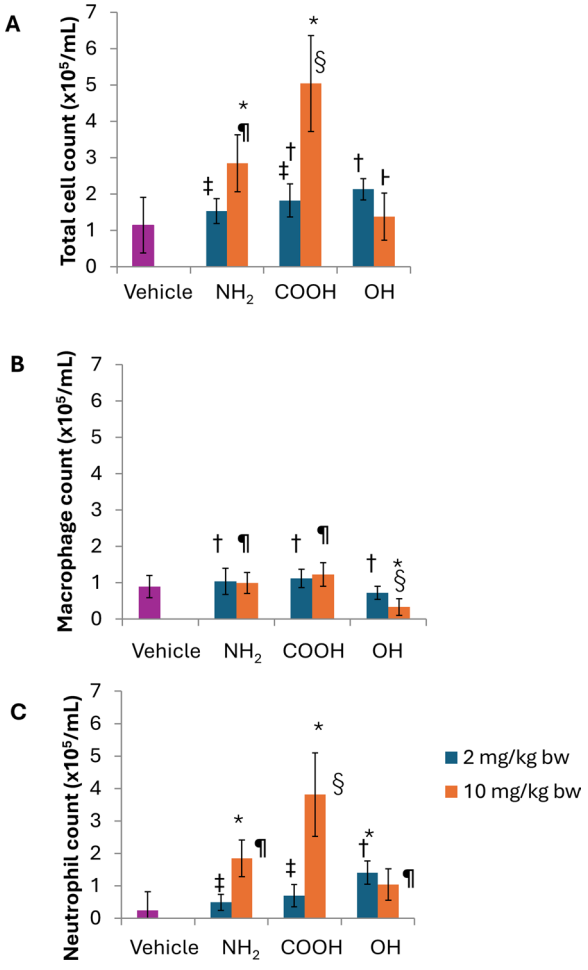

Fig. 1 BALF total and differential cell count in mice exposed to SiO_2NPs for 24 h via pharyngeal aspiration. OH-, COOH- and NH_2-functonalized rhodamine-labeled SiO_2NPs by pharyngeal aspiration at 2 or 10 mg/kg bw. At 24 h after the treatment, BALF was collected and total and differential cell counts were determined using Differential Quick Stain Kit and hematocell counter. About 400 cells in three fields were counted on a slide from one animal each. Data are mean ± SD (n = 6 each) **A** BALF total cell count. **B** BALF macrophage cell count. **C** BALF neutrophil cell count. *P < 0.05, compared with the vehicle group, by ANOVA followed by Dunnett multiple comparison test. There is a significant difference between the different types of SiO_2NPs at the same concentration, which are not marked by the same symbols (§,¶,‡ and†,‡)

OH-SiO_2NPs induced a greater increase in BALF neutrophils COOH- or NH_2-SiO_2NPs at the low dose

To evaluate NPs-induced lung inflammatory response, BALF was collected for total and differential cell counts. At 2 mg/kg bw, any type of SiO_2NPs did not significantly change BALF total cell (Fig. 1A) or macrophage count (Fig. 1B), while only OH- SiO_2NPs, significantly increased BALF neutrophil count (Fig. 1C).

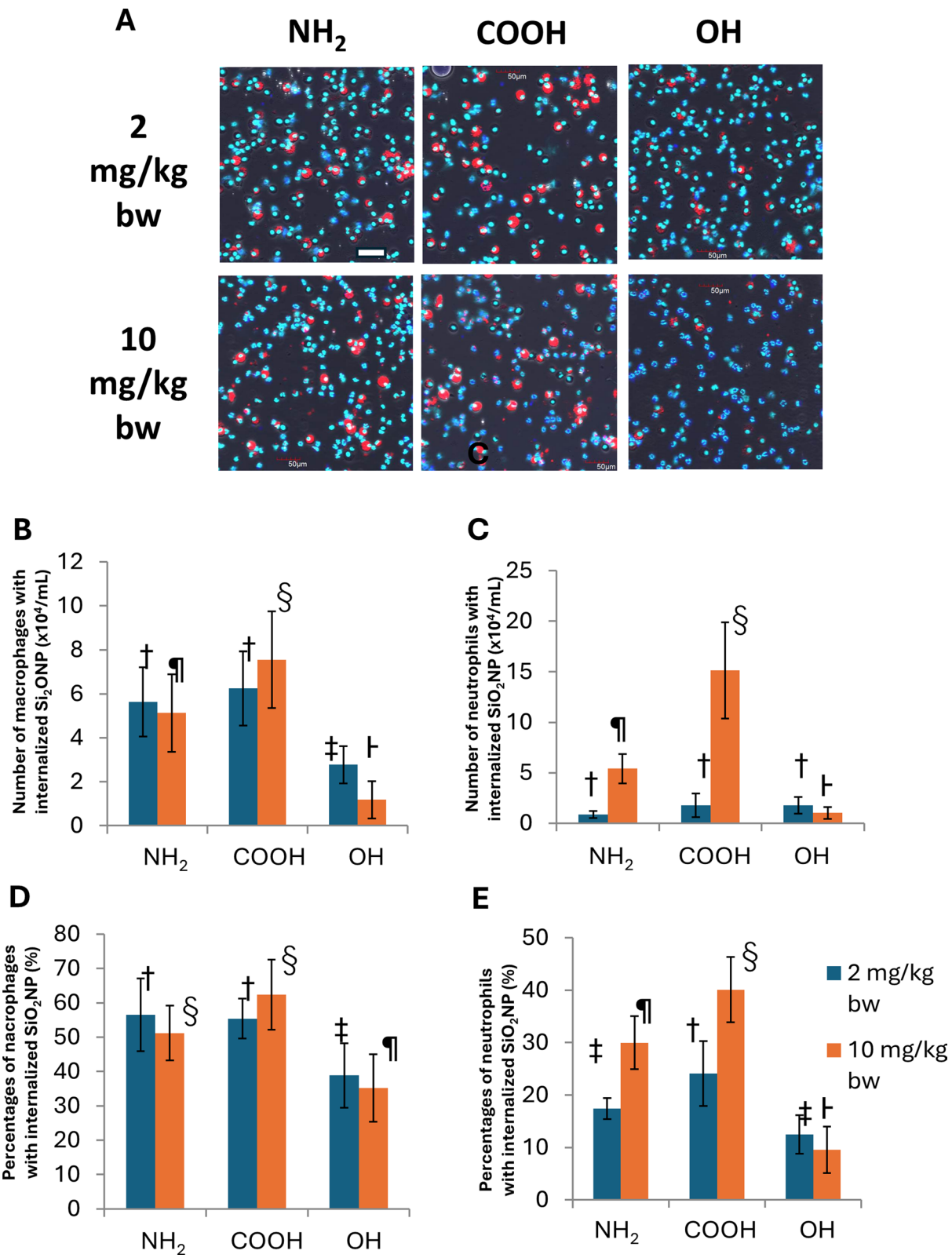

Fig. 2 (See legend on next page.)

(See figure on previous page.)

Fig. 2 OH-, NH_2- or COOH-SiO_2NPs internalized in macrophages and neutrophils in BALF collected from mice exposed to each ofthese NPs by pharyngeal aspiration. At 24 h after the treatment, BALF was collected and cytospinned on slides. **A** Confocal images of the cells recovered from BALF and stained using Differential Quick Stain Kit. Rhodamine-labelled SiO_2NPs are stained red, while the nuclei and cytoplasm are stained dark blue and light blue, respectively. Scale bars = 50 µm. **B** Count of macrophages with internalized rhodamine-labelled SiO_2NPs. All 71–576 cells in three fields on the slide from each animal were counted. **C** Counts of neutrophils with internalized rhodamine-labelled SiO_2NPs. All 0–490 cells in three fields on the slide from each animal were counted. **D** Percentage of the macrophages with internalized NPs relative to the total number of macrophages. **E** Percentage of neutrophils with internalized NPs relative to the total neutrophils. ANOVA followed by Tukey multiple comparison test was used to determine the significance of the differences between the different types of SiO_2NPs at the same concentration. There is a significant difference between the different types of SiO_2NPs at the same concentration, which are not marked by the same symbols (§,¶,Ŧ and†,‡). Significance level was set at 5%

COOH-SiO_2NPs increased BALF neutrophils to a greater extent than NH_2-or OH-SiO_2NPs at the high dose

At 10 mg/kg bw, COOH-SiO_2NPs induced the largest increase in BALF macrophage count (Fig. 1B), and NH_2- and COOH-SiO_2NPs each significantly increased total BALF cell and neutrophil counts (Fig. 1A and C), while OH- SiO_2NPs significantly decreased BALF macrophage count (Fig. 1B). Multiple regression analysis showed significant interaction between type of SiO_2NPs and dose for BALF total cell or neutrophil count, but not for macrophage count (Suppl. Table 1), indicating significant effect of type of SiO_2NPs on the intensity or direction of SiO_2NPs -induced change in BALF total cell or neutrophil count. Additional multiple regression analysis without interaction showed significant effect of type of SiO_2NPs in BALF macrophage count. These results suggest that OH- SiO_2NPs induced lung inflammatory response marked by neutrophil accumulation at low dose and reduced BALF macrophages at high dose.

Fewer macrophages and neutrophiles with internalized OH-SiO_2NPs

To determine the impact of the functional groups on the fate of NPs after pharyngeal aspiration, the macrophages and neutrophils were differentially stained and examined by confocal microscopy. COOH- and NH_2- SiO_2NPs were internalized in macrophages regardless of the dose, while internalization of OH-SiO_2NPs in the macrophages was less pronounced (Fig. 2A). Quantitative analysis confirmed that around 60% of macrophages showed internalization of NH_2- and COOH- SiO_2NPs at 2 and 10 mg/kg bw, compared with less than 40% for OH-SiO_2NPs (Fig. 2B and C). With regard to neutrophils, the numbers or percentages of neutrophils that showed COOH- and NH2-SiO_2NPs internalization increased dose-dependently, but no such dose-dependent increase was noted for OH-SiO_2NPs (Fig. 2D and E). Multiple regression analysis showed significant interaction between type of SiO_2NPs and dose in multiple regression model for the number of macrophages with internalized SiO_2NPs and the number or percentage of neutrophils with internalized SiO_2NPs, indicating significant effect of type of SiO_2NPs on the intensity or direction of SiO_2NPs -induced change in the above responses, but not for the percentage of macrophages with internalized SiO_2NPs (Suppl. Table 2). Additional multiple regression analysis without interaction showed significant effect of type of SiO_2NPs. These results suggest a weaker in vivo OH- SiO_2NPs internalization in macrophages and neutrophiles.

In vitro experiments

OH-SiO_2NPs is the most toxic to cultured murine RAW264.7 macrophages

Since OH-SiO_2NPs dose-dependently decreased BALF macrophages (Fig. 1B), we updated our hypothesis: that OH-SiO_2NPs are the most cytotoxic NPs. To test this hypothesis, we conducted MTS cell viability assay and LDH cytotoxicity assay for the three SiO_2NPs in RAW264.7 macrophage cell line. Treatment of these cells with OH- SiO_2NPs, but not NH_2- and COOH- SiO_2NPs, significantly decreased cell viability measured by MTS, in time- and dose-dependent manners (Fig. 3 and Suppl. Figure 1). Multiple regression analysis showed significant interaction between type of SiO_2NPs and dose, both after 4 h and 24 h exposure, indicating significant effect of type of SiO_2NPs on the intensity of SiO_2NPs -induced decrease in MTS cell viability (Suppl. Table 3). The LDH cytotoxicity test also showed higher LDH release from cells exposed to OH-NPs compared to the other types of NPs (Suppl. Figure 2). Since OH-SiO_2NPs caused the greatest reduction in MTS cell viability among the tested particles, we evaluated the potential interference of OH-SiO_2NPs in the MTS assay, including possible absorbance generation by the nanoparticles themselves, inhibition of formazan formation, or alteration of formazan absorbance. The results showed no evidence of interference by OH-SiO_2NPs at concentrations ranging from 0.3 to 30 µg/cm^2 (Suppl. Figure 3). These results are in agreement with those of the in vivo experiments and suggest that OH-SiO_2NPs are the most toxic particles to murine RAW264.7 macrophage cell line, and that NH_2- and COOH-functionalization mitigated this harmful effect.

Weaker OH-SiO_2NPs internalization into RAW264.8 than NH_2-SiO_2NPs

Next, we assessed the internalization of the three types of NPs into RAW264.8 macrophages in order to understand how internalization is associated with OH- SiO_2NPs toxicity. Confocal microscopy showed that OH-SiO_2NPs were mainly localized in the plasma membrane of

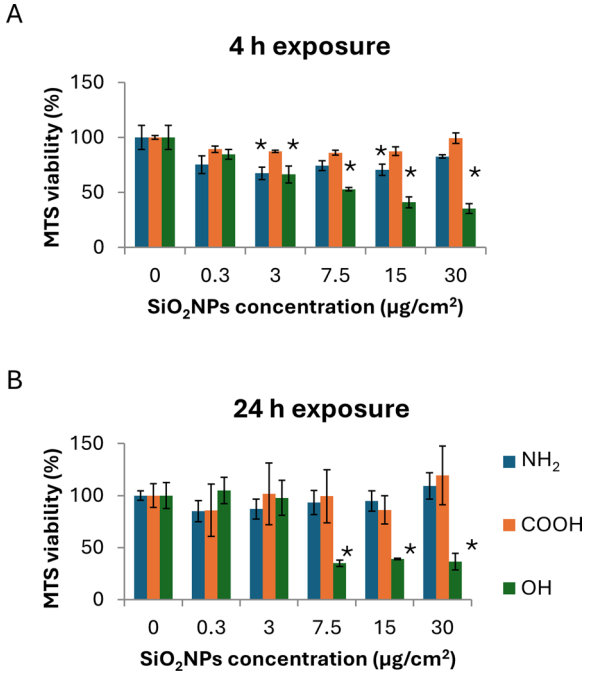

Fig. 3 Viability of RAW264.8 cells, as determined by MTS, at 4 or 24 h after treatment with SiO_2NPs at the indicated concentrations. RAW264.8 cells were treated with OH-, NH_2 or COOH-modified rhodamine-labelled SiO_2NPs dispersed in the cell culture medium at 0.3 to 30 µg/cm^2 (1–100 µg/mL). After the treatment, cell viability was assessed by measuring absorbance at 490 nm, which reflected the reduction of {3-(4,5-dimethylthiazol-2-yl)-5-(3-carboxymethoxyphenyl)-2-(4-sulfophenyl)-2H-tetrazolium} (MTS) to formazan by mitochondria in viable cells. Data are mean ± SD (n = 6). *P < 0.05, compared with untreated control (0 µg/cm^2), by Dunnett's test following ANOVA

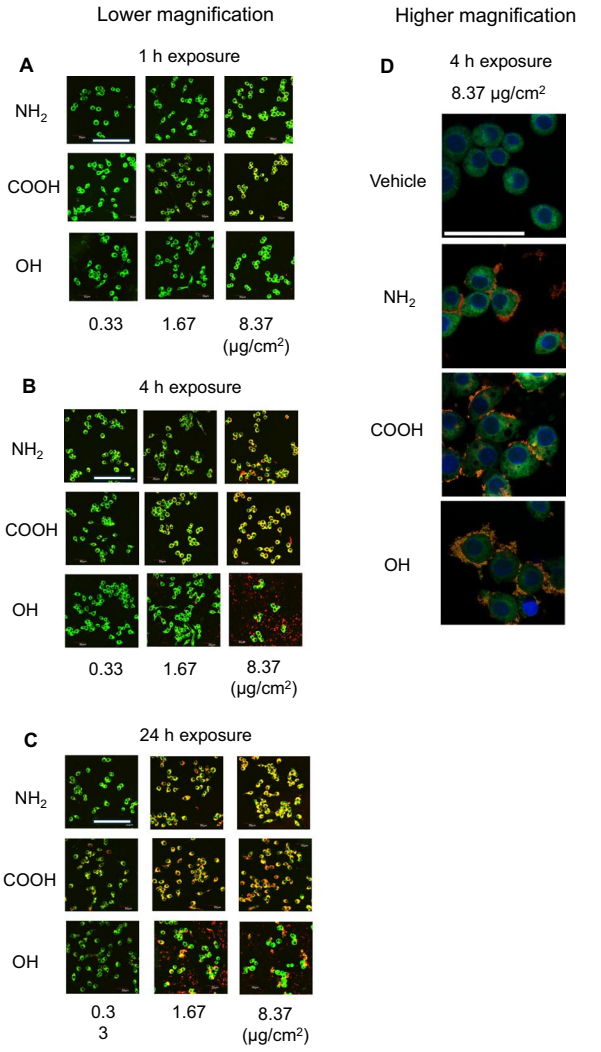

Fig. 4 Colocalization of SiO_2NPs in RAW264.8 macrophages exposed to OH-, NH_2- or COOH-SiO_2NPs for 1, 4 and 24 h. RAW 264.8 cells were exposed to different concentrations of the three types of SiO_2NPs for **A** 1 h, (**B**, **D**) 4 h, and (**C**) 24 h. Internalization of NPs in the cells was assessed by confocal microscopy. Green – plasma membrane, red – SiO_2NPs. Scale bars = 100 µm. The magnification is the same in all photomicrographs of (**A**), (**B**), and (**C**), and in all photomicrographs of (**D**). Magnification of objective lens is × 63 for (**A**), (**B**), (**C**) and × 100 for (**D**)

RAW264.8 macrophages, irrespective of the dose used (Fig. 4A, B, C and D). This was remarkable after 1 h of treatment at the largest concentration of NPs and even more prominent after 4 and 24 h of treatment. These results suggest weaker OH- SiO_2NPs internalization into RAW264.8 macrophage cell line, which are in agreement with the results of the in vivo experiments and implied that internalization of these NPs does not play a role in their toxicity.

Confirmation of weaker OH-SiO_2NPs internalization by flow cytometry

Internalization of NPs into the cells was further quantified by flow cytometry (Fig. 5 and Suppl. Figures 4). To eliminate any signal originating from NPs adsorbed on the surface of the cells, 0.1% trypan blue was added shortly before the analysis. The working concentration of trypan blue was optimized in a series of preliminary experiments (Suppl. Figure 4). Flow cytometry identified three populations of RAW264.4 cells, designated as gates A, B, and C, showing distinct forward scatter (FS) signals that reflected differences in cell size (Suppl. Figure 5). Because the slopes of the regression lines, with rhodamine intensity as the dependent variable and SiO_2NP concentration as the independent variable, differed among SiO_2NP types (Suppl. Figure 6), the rhodamine intensities of COOH-SiO_2NPs and OH-SiO_2NPs were normalized by dividing each value by the ratio of their respective slope to that of NH_2-SiO_2NPs, yielding the relative rhodamine intensity for comparison. Exposure to COOH-, NH_2- and OH-SiO_2NPs increased the mean value of the normalized fluorescence intensity in the population gated to A, B and C (Fig. 5 and Suppl. Figure 4), and such increase was dose-dependent.

Following exposure of the cells to the three types of SiO_2NPs at 0.33 µg/cm^2 (representing the non-cytotoxic

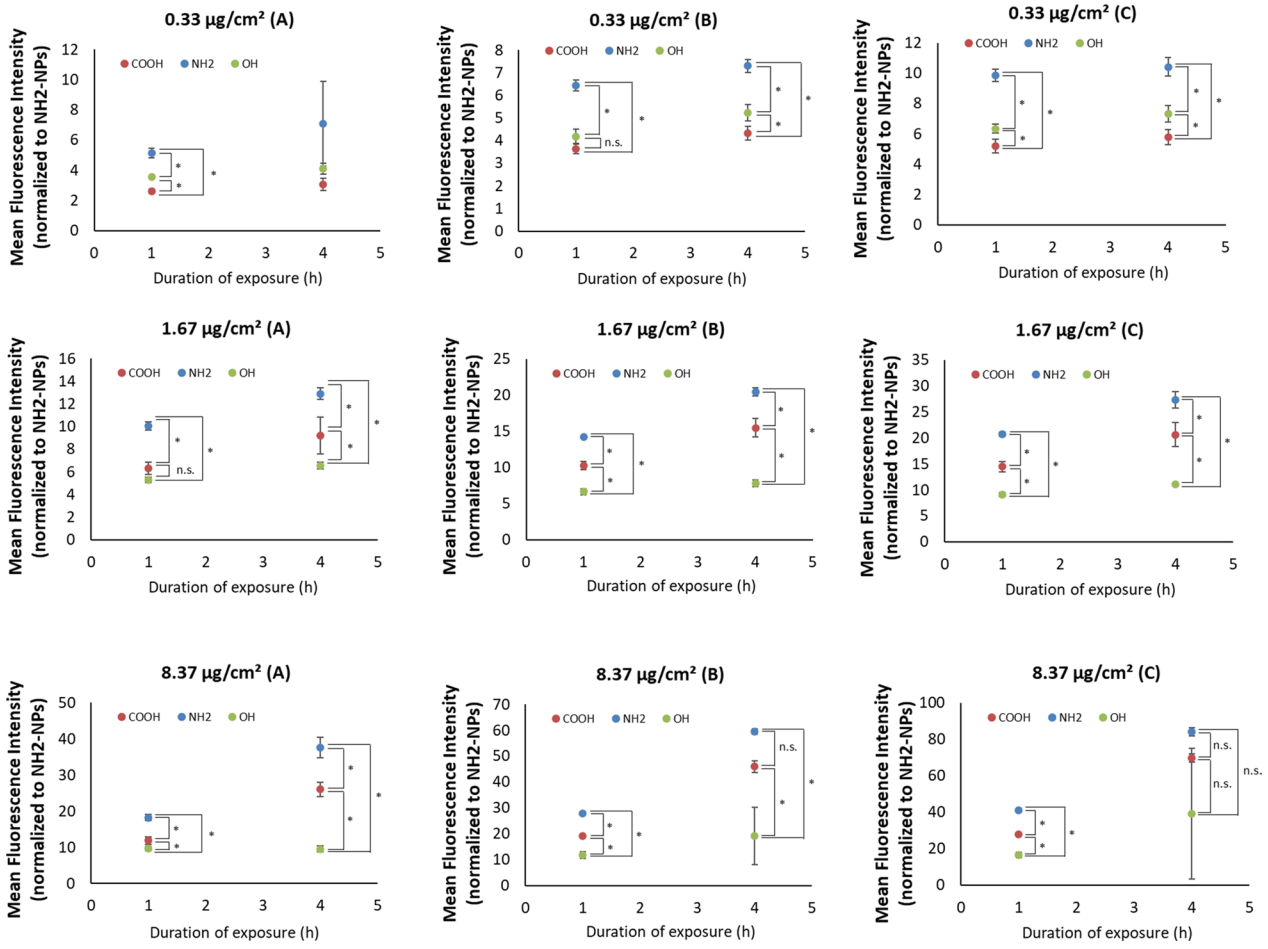

Fig. 5 Assessment of internalization of SiO_2NPs into RAW264.8 cells by flow cytometry. Cells were exposed to different concentrations of NPs (0.33, 1.67, and 8.37 mg/cm^2) for 1h or 4 h. After the treatment, the cells were washed and incubated with 0.1% trypan blue for 1 min, in order to quench fluorescence emanating from NPs adsorbed on the surface of the cells. Mean fluorescence intensity of the cells was analyzed using excitation/emission wavelengths set corresponding to rhodamine dye. Data are MFI ± SD (n = 3, 10,000 cells were analyzed per sample). ANOVA followed by Tukey multiple comparison test was applied to test for differences among the three types of SiO_2NPs (*P < 0.05). *n.s* not significant

level of OH-SiO_2NPs, measured by the MTS assay), for 1 or 4 h, the mean relative rhodamine intensity for the population gated to A, B and C was higher in the order of NH2- > OH- > COOH-SiO_2NPs. However, at 1.66 or 8.37 µg/cm^2 for 1 or 4 h, the mean relative rhodamine intensity was higher in the order of NH2- > COOH- > OH-SiO_2NPs. Specifically, for 1.66 and 8.37 µg/cm^2, the mean relative rhodamine intensity increased time-dependently for NH_2 and COOH-SiO_2NPs, but the time-dependent increase was suppressed for OH-SiO2NPs (Fig. 5). The results of flow cytometry confirmed weaker OH-SiO_2NPs internalization into RAW264.7 macrophages, compared with COOH- and NH_2- SiO_2NPs.

Co-treatment with apoptosis and necroptosis inhibitors partially suppresses OH-SiO_2NPs-induced cell viability

Next, we determined the cell death signaling involved in the cytotoxic effect of OH-SiO_2NPs on RAW264.7 cells, using MTS assay with pan caspase, necroptosis, pyroptosis and autophagy inhibitors. No change in cell viability was noted in the presence OH-SiO_2NPs and any of these inhibitors alone for 18 h (Fig. 6A, B, C and D), suggesting that OH-SiO2NPs cytotoxicity is not explained by apoptosis, necroptosis, pyroptosis or autophagy. However, the OH-SiO_2NPs' cytotoxic effect on cultured RAW264.7 cells was partially reduced in the combined presence of pan-caspase inhibitor and necroptosis inhibitor (Fig. 6E). Finally, DAPI nuclear staining of RAW264.7 cells exposed to 8.37 µg /cm^2 (28 µg/mL) OH-SiO_2NPs did not show nuclear fragmentation but showed chromatin condensation (Fig. 7). These results suggest that OH- SiO_2NPs-induced reduction in cell viability is not due to typical apoptosis of RAW264.7 cells.

Upregulation of IL-1β and TNFα by OH-SiO2NPs in RAW264.8 macrophages

Our in vivo experiments showed that pharyngeal aspiration of NPs in mice induced lung weight changes

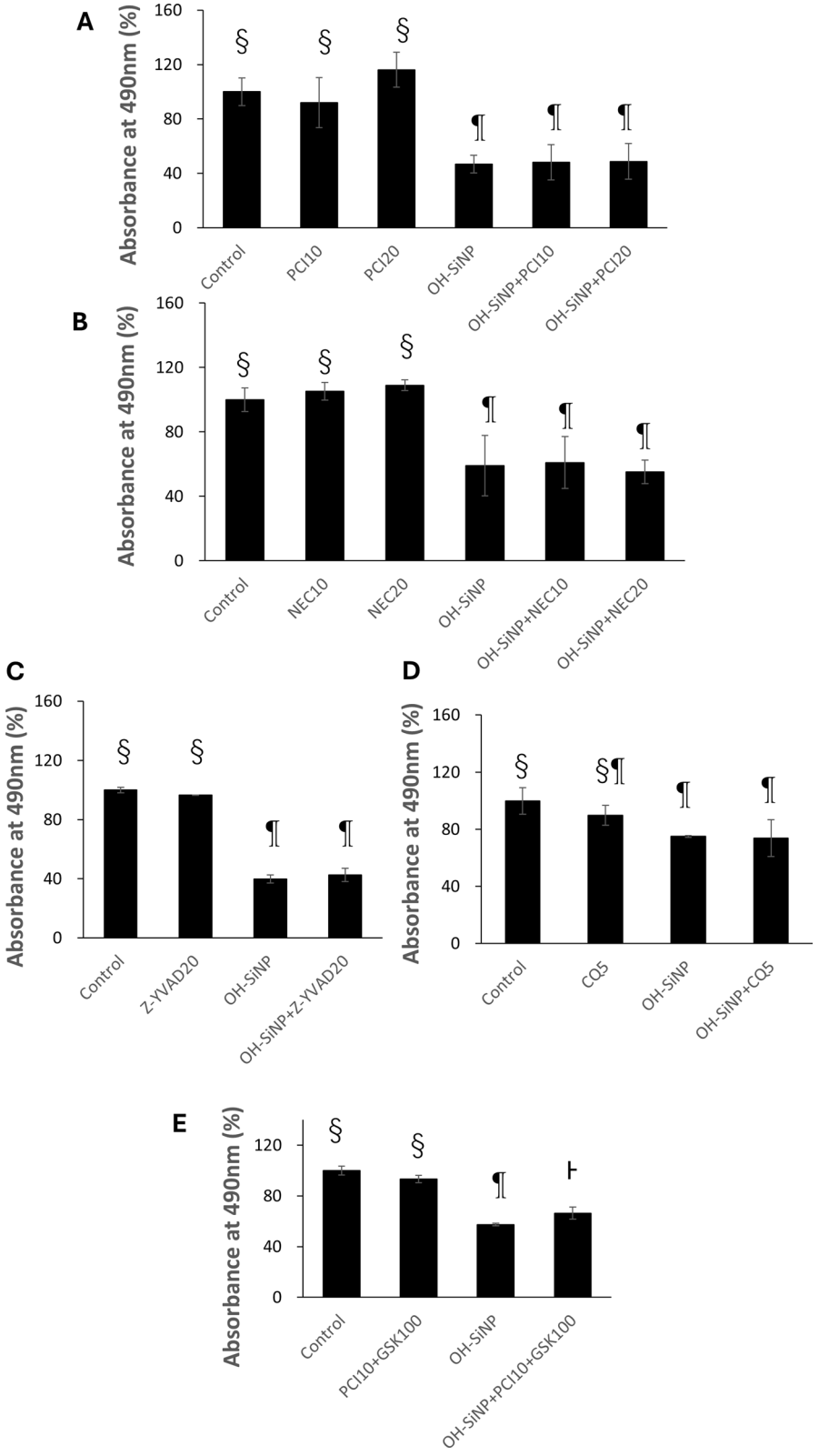

Fig. 6 (See legend on next page.)

(See figure on previous page.)

Fig. 6 Effect of treatment with inhibitors of pan-caspase, necroptosis, pyroptosis, and autophagy and co-treatment with pan-caspase inhibitor and necroptosis inhibitor on MTS cytotoxicity of OH-SiO_2NPs in vitro. There is a significant difference between the different treatments, which are not marked by the same symbols (§,¶,Ŧ) (by Tukey- Kramer method following ANOVA.). Significance level was set at 5%. **A** Effect of pan-caspase inhibitor Z-VAD-FMK on MTS viability of cells exposed to OH-SiO_2NPs. RAW264.1 cells were preincubated with 20 or 40 μM of pan-caspase inhibitor Z-VAD-FMK or vehicle for one hour, and exposed to OH-SiO_2NPs at 8.37 μg/cm^2 (28 μg/mL) for 18 h. Cytotoxicity was evaluated using CellTiter 96® Aqueous One Solution Cell Proliferation Assay (Promega). Concentrations of inhibitors larger than 20 μM were not used due to their cell toxicity. PCI: pan caspase inhibitor (Z-VAD-FMK), 20: 20 μM, 40: 40 μM. **B** Effect of necroptosis inhibitor necrostatin-1 (RIP1-specific inhibitor) on MTS viability of cells exposed to OH-SiO_2NPs. RAW264.1 cells were preincubated with necrostatin-1 at 10 or 20 μM for one hour, and exposed to OH-SiO_2NPs at 8.37 μg/cm^2 (28 μg/mL) for 18 h. Cytotoxicity was evaluated using CellTiter 96® Aqueous One Solution Cell Proliferation Assay (Promega). Concentrations of inhibitors larger than 20 μM were not used due to their cell toxicity. *NEC* necrostatin-1(RIP1 kinase inhibitor), 10: 10 μM, 20: 20 μM **C** Effect of pyroptosis inhibitor Z-YVAD-FMK (caspase-1 and -4 inhibitor) on MTS viability of cells exposed to OH-SiO_2NPs. RAW264.1 cells were preincubated with Z-YVAD-FMK inactive control at 20 μM for one hour, and exposed to OH-SiO_2NPs at 8.37 μg/cm^2 (28 μg/mL) for 18 h. Cytotoxicity was evaluated using CellTiter 96® Aqueous One Solution Cell Proliferation Assay (Promega). Concentrations of inhibitors larger than 20 μM were not used due to their cell toxicity. Z-YVAD: Z-YVAD-FMK, 20: 20 μM **D** Effect of autophagy inhibitor chloroquine disphosphate (inhibitor of autophagosome-lysosome fusion) on MTS viability of cells exposed to OH-SiO_2NPs. RAW264.1 cells were preincubated with chloroquine diphosphate at 5 μM for one hour, and exposed to OH-SiO_2NPs at 8.37 μg/cm^2 (28 μg/mL) for 18 h. Cytotoxicity was evaluated using CellTiter 96® Aqueous One Solution Cell Proliferation Assay (Promega). Concentrations of inhibitors larger than 5 μM were not used due to their cell toxicity. CQ: Autophagy inhibitor, chloroquine diphosphate, 5: 5 μM **E** Effect of co-treatment with pan-caspase inhibitor Z-VAD-FMK and necroptosis inhibitor GSK'963 (RIP1-specific inhibitors) on MTS viability of cells exposed to OH-SiO_2NPs. RAW264.1 cells were preincubated with Z-VAD-FMK at 10 μM and GSK'963 at 100 μM for one hour, and exposed to OH-SiO_2NPs at 8.37 μg/cm^2 (28 μg/mL) for 18 h. Cytotoxicity was evaluated using CellTiter 96® Aqueous One Solution Cell Proliferation Assay (Promega). Concentrations of pan-caspase inhibitor or necroptosis inhibitor larger than10 or 100 μM were not used due to their cell toxicity. PCI: pan caspase inhibitor (Z-VAD-FMK), GSK: GSK'963 (necroptosis inhibitor/RIP1 kinase inhibitor)

associated with BALF inflammatory cell accumulation. Accordingly, we assessed the effects of these NPs on the expression of pro-inflammatory cytokines or chemokines using our in vitro model of RAW264.8 macrophages and qRT-PCR. Since exposure to OH-SiO_2NPs increased BALF neutrophils at the low dose, the expressions of macrophage inflammatory protein-2 (MIP-2), which is known to recruit and activate neutrophils [33], and monocyte chemoattractant protein-1 (MCP-1), which recruits both neutrophils and monocytes [34], were measured. We evaluated the mRNA expression levels of cytokines and chemokines rather than their protein secretion, as the protein concentrations in the culture medium were near the detection limit of the commercially available ELISA kits. Exposure of the RAW264.8 cell line to SiO_2NPs at 8.37 μg/cm^2 for one hour significantly increased the mRNA level of MIP-2 in the order of OH- = NH2- > COOH-SiO_2NPs (Table 4). Furthermore, exposure to OH- or NH2-SiO_2NPs for one hour significantly increased the mRNA level of MCP-1 in the order of OH- > NH_2- SiO_2NPs. Multiple regression analysis showed significant interaction between type of SiO_2NPs and dose for all of the examined genes, indicating significant effect of type of SiO_2NPs on the intensity of SiO_2NPs-induced upregulation of the examined gene expression (Suppl. Table 4). Exposure to these SiO_2NPs at 8.37 μg/cm^2 for 4 h resulted in further increase in the mRNA levels of MIP-2 and MCP-1 but the effect of SiO_2NPs became insignificant. The mRNA level of IL-1β increased significantly during exposure to OH- SiO_2NPs at 8.37 μg/cm^2 for one hour but decreased during exposure to NH_2- and COOH- SiO_2NPs (Table 5). On the other hand, the mRNA level of TNF-α significantly increased after exposure to all three types of SiO_2NPs at 8.37 μg/cm^2 for one hour and the increase was in the order of OH- > NH2- > COOH- SiO_2NPs. However, the extent of IL-1β and TNF-α upregulation was smaller by 4-h exposure irrespective of the type of NPs and the differences in the upregulated levels among the three NPs became insignificant at 1.66 and 8.37 μg/cm^2. Multiple regression analysis showed no significant interaction between type of SiO_2NPs and dose, indicating no effect of type of SiO_2NPs on the intensity or direction of change in the expression of the examined genes (Suppl. Table 4). Considered together, the above results suggest that the cytotoxic effects of SiO_2NPs pharyngeal aspiration include lung inflammation and cell death through apoptotic and necroptotic pathways, and that the former is linked with the upregulation of pro-inflammatory cytokines.

Discussion

NH_2- and COOH-functionalization of OH-SiO_2NPs reduced OH-SiO_2NPs-induced increase in lung weight

Exposure to OH-SiO_2NPs at 2 and 10 mg/kg bw induced the largest increase in lung weight compared to the other two SiO_2NPs. Increased lung weight can reflect pulmonary inflammation, which is associated with intense protein/fluid leakage from the vasculature into the alveoli mediated by inflammatory signals from pulmonary cells [35].

At the high dose, COOH-SiO_2NPs induced a greater infiltration of BALF neutrophils than NH_2- or OH-SiO_2NPs, whereas COOH or NH_2 functionalization attenuated OH-SiO_2NP-induced neutrophil infiltration at the low dose

With regard to BALF cells, our results showed that the type of the response to exposure was dose-and NP-functionalization-dependent. Thus, at 10 mg/kb bw, COOH-SiO_2NPs significantly increased BALF macrophages and

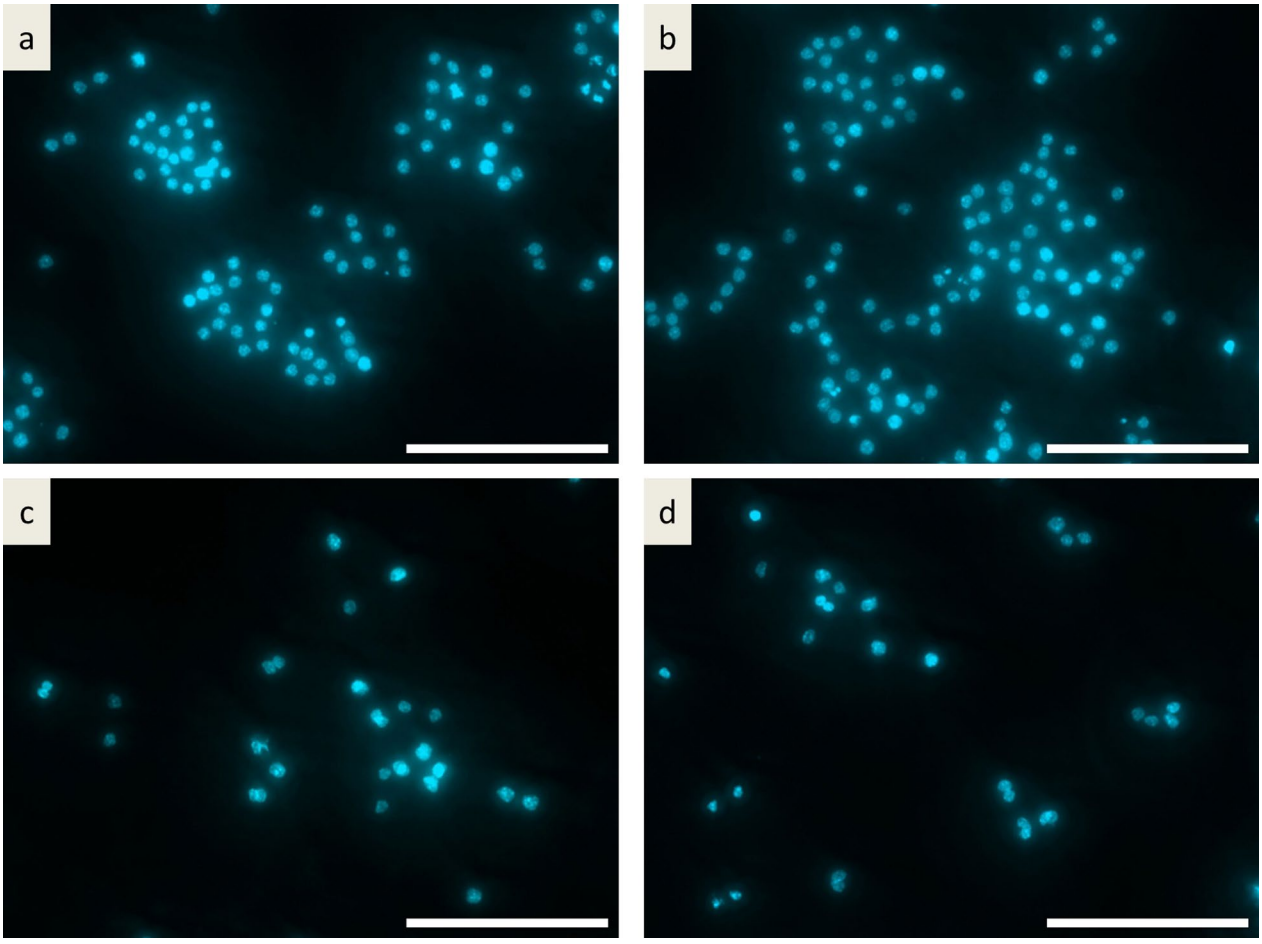

Fig. 7 Fluorescence image of RAW264.7 nuclei stained by DAPI. We examined nuclear morphology to determine whether 28 μg/cm$_2$ OH-SiNP can induce apoptosis of RAW264.7. Note the lack of signs of apoptosis (e.g., nuclear fragmentation or chromatin limbing) in the presence of OH-SiO_2NPs **a**, **b** RAW264.7 cells exposed to the culture medium only for 18 h, **c**, **d** RAW264.7 cells exposed to OH-SiO_2NPs at 8.37 μg /cm^2 (28 μg/mL) for 18 h. Scale bars = 100 μm

neutrophils, NH_2-SiO_2NPs significantly increased BALF neutrophils, and in contrast, OH-SiO_2NPs significantly decreased BALF macrophages. On the other hand, at 2 mg/kg bw, OH-SiO_2NPs increased BALF neutrophiles, while COOH- and NH_2-SiO_2NPs did not. The response of BALF cells at 2 mg/kg bw might be linked with cytotoxicity of OH-SiO_2NPs. OH-SiO_2NPs-induced decrease in macrophages or the lack of increase in neutrophils at 10 mg/kg bw could possibly be due to cell death.

Surface modification of OH-SiO_2NPs reduces its cytotoxicity against RAW264.7 macrophage

Our in vitro studies demonstrated that OH-SiO_2NPs, but not the other two types of NPs, dose-dependently decreased the viability of RAW264.7 macrophages. Specifically, exposure to OH-SiO_2NPs at ≥ 3 mg/cm^2 for 4 h significantly decreased cell viability, while exposure to the same NPs at larger dose (≥ 7.5 mg/cm^2) for 24 h significantly decreased the cell viability. This discrepancy in the lowest level for cytotoxicity between 4- and 24-h exposure may be explained by proliferation of the cells after the 4-h exposure. This argument is supported by the higher absorbance at 24 h than at 4 h (Suppl. Figure 6). The results suggest that surface modification of OH-SiO_2NPs reduced its cytotoxicity against murine macrophages, which might also explain the in vivo results that showed the uniqueness of OH-SiO_2NPs in dose-dependently reducing BALF macrophages and increasing lung weight. The present results are consistent with previous studies. Non-functionalized StÖber colloidal silica exhibited higher cytotoxicity toward RAW264.7 cells than amine-modified StÖber colloidal silica [36]. Similarly, Lankoff et al. reported that unmodified SiO_2NPs induced greater cytotoxicity and genotoxicity in human peripheral lymphocytes than aminopropyl- or vinyl-modified SiO_2NPs [24]. The suppression of particle-induced cytotoxicity through surface modification has also been observed for 1000 nm amorphous SiO_2 particles [37] and mesoporous silica SBA-15[38]. However, the opposite trend was reported for amino- or carboxyl- modified

Table 4 Relative mRNA levels of MIP-2 and MCP-1in RAW264.1 cells exposed to the three types of SiO_2NPs

		Concentration (μg/cm^2)	0	0.33		1.67		8.37	
	Duration of exposure (h)								
MIP-2	1	Vehicle	0.66 ± 0.02						
(× 10^{-1})		NH_2-SiO_2NPs		0.49 ± 0.03	§	0.77 ± 0.09	§	9.46 ± 0.99*	§
		COOH-SiO_2NPs		0.60 ± 0.17	§	0.67 ± 0.08	§	5.39 ± 1.02*	
		OH-SiO_2NPs		0.45 ± 0.13	§	0.70 ± 0.07	§	9.01 ± 2.02*	§
	4	Vehicle	0.31 ± 0.05						
		NH_2-SiO_2NPs		0.28 ± 0.17	§¶	22.0 ± 36.7	§	57.1 ± 49.2	§
		COOH-SiO_2NPs		0.46 ± 0.00	§	1.02 ± 0.29	§	35.0 ± 7.1*	§
		OH-SiO_2NPs		0.08 ± 0.05	¶	0.85 ± 0.26	§	62.4 ± 7.7*	§
MCP-1	1	Vehicle	1.01 ± 0.16						
		NH_2-SiO_2NPs		0.55 ± 0.05*	§	0.62 ± 0.05*	§	1.74 ± 0.11*	§
		COOH-SiO_2NPs		0.51 ± 0.02*	§	0.65 ± 0.08*	§	1.29 ± 0.21	¶
		OH-SiO_2NPs		0.93 ± 0.11	¶	0.84 ± 0.05	¶	2.18 ± 0.27*	§
	4	Vehicle	0.33 ± 0.07						
		NH_2-SiO_2NPs		0.26 ± 0.01	§	1.89 ± 2.64	§	4.40 ± 3.59	§
		COOH-SiO_2NPs		0.27 ± 0.01	§¶	0.35 ± 0.03	§	2.86 ± 0.91	§
		OH-SiO_2NPs		0.33 ± 0.05	¶	0.35 ± 0.03	§	4.10 ± 0.45*	§

MIP-2 and MCP-1 mRNA levels relative to geometric mean of β-actin and GAPDH mRNA, and 18S rRNA level

Data are mean ± SD (n = 3, each). Asterisk (*) denotes significant difference with the vehicle control (by Dunnett's multiple comparison following ANOVA). There is a significant difference between the different types of SiO_2NPs at the same concentration, which are not marked by the same symbols (§ or ¶) (by Tukey–Kramer multiple comparison following ANOVA). Significance level was set at 5%

Table 5 Relative mRNA levels of IL-1β and TNF-α in RAW264.1 cells exposed to the three types of SiO_2NPs

		Concentration (μg/cm^2)	0	0.33		1.67		8.37	
	Duration of exposure (h)								
IL-1β	1	Vehicle	2.35 ± 0.16						
		NH_2-SiO_2NPs		1.08 ± 0.11	§	1.31 ± 0.25*	§	1.88 ± 0.32*	§
		COOH-SiO_2NPs		0.90 ± 0.25*	§	1.27 ± 0.21*	§	1.57 ± 0.27*	§
		OH-SiO_2NPs		2.07 ± 0.16	¶	1.12 ± 0.09	§	3.61 ± 0.76*	¶
	4	Vehicle	0.78 ± 0.21						
		NH_2-SiO_2NPs		0.74 ± 0.05	§	2.06 ± 1.34	§	1.25 ± 0.69	§
		COOH-SiO_2NPs		0.83 ± 0.08	§	0.82 ± 0.27	§	0.30 ± 0.11*	§
		OH-SiO_2NPs		1.31 ± 0.11	¶	1.56 ± 0.44	§	0.92 ± 0.15	§
							§		
TNF-α	1	Vehicle	1.14 ± 0.04						
		NH_2-SiO_2NPs		1.00 ± 0.06	§	1.07 ± 0.09	§	1.57 ± 0.07*	§
		COOH-SiO_2NPs		0.93 ± 0.10*	§	1.00 ± 0.04	§	1.35 ± 0.10*	¶
		OH-SiO_2NPs		1.05 ± 0.08	§	0.98 ± 0.09*	§	2.02 ± 0.04*	†
	4	Vehicle	0.63 ± 0.05						
		NH_2-SiO_2NPs		0.60 ± 0.01	§	1.09 ± 0.43	§	1.29 ± 0.38	§
		COOH-SiO_2NPs		0.63 ± 0.06	§	0.75 ± 0.01	§	1.18 ± 0.15*	§
		OH-SiO_2NPs		0.82 ± 0.04	¶	0.83 ± 0.10	§	1.28 ± 0.17*	§

IL-1β and TNF-α mRNA levels relative to geometric mean of β-actin and GAPDH mRNA, and 18S r RNA level

Data are mean ± SD (n = 3, each). Asterisk (*) denotes significant difference with the vehicle control (by Dunnett's multiple comparison following ANOVA). There is a significant difference between the different types of SiO_2NPs at the same concentration, which are not marked by the same symbols (§, ¶ or †) (by Tukey–Kramer multiple comparison following ANOVA). Significance level was set at 5%

SBA-15-type silica synthesized via a co-condensation route using ethanol [39].

Internalization of SiO_2NPs in RAW264.7 macrophages does not explain OH-SiO_2NP toxicity

Our in vivo experiments showed a lower percentage of macrophages and neutrophiles internalized OH-SiO_2NPs compared with NH_2- and COOH-SiO_2NPs. This finding was consistent with our in vitro results, in which flow cytometric quantification revealed less internalization of OH-SiO_2NPs. Confocal microscopy of RAW264.8 macrophages also confirmed less cellular uptake of OH-SiO_2NPs ithan of NH_2- and COOH-SiO_2NPs. Taken together with the observation that OH-SiO_2NPs

exhibited the highest cytotoxicity, these results suggest that internalization of OH-SiO_2NPs is unlikely to be the primary mechanism underlying OH-SiO_2NP-induced cytotoxicity. Similarly, in the study by Lankoff et al. [24], side scatter (SSC) signals in flowcytometry-an indicator of nanoparticle binding and uptake-were highest for aminopropyl-modified SiO_2NPs, followed by unmodified and then vinyl-modified SiO_2NPs [24]. This order differs from that of cytotoxicity, further supporting the lack of correlation between cellular uptake and toxicity of SiO_2NPs. However, internalization may be a prerequisite for cytotoxicity induced by micron-sized particles, as a previous study demonstrated that inhibitors of lysosomal function, such as CA-074-Me (a cathepsin B inhibitor) and bafilomycin A (a vacuolar-type ATPase inhibitor), suppressed the cytotoxicity of 1000 nm amorphous silica particles, indicating the involvement of lysosomes in their toxicity [25].

Does localization of OH-SiO_2NPs near cell membrane play a role in cytotoxicity?

Confocal microscopy of RAW264.7 macrophages revealed more distinct colocalization of OH-SiO_2NPs with the cell membrane compared with NH_2– or COOH-SiO_2NPs. This observation is consistent with a previous study showing that non-functionalized Stöber colloidal silica exhibits higher cytotoxicity and greater cellular association-measured as the mass of silicon per protein extracted from cells incubated with silica nanoparticles-than amine-modified Stöber silica [36]. These findings suggest an important contribution of physical contact between particles and the cell membrane to cytotoxicity. Recent studies have highlighted the role of surface silanol groups in the cytotoxicity of pyrogenic amorphous SiO_2NPs, including reports of cytolytic toxicity associated with silanol-rich particles[40], membranolysis driven by nearly free surface silanols [41], and the critical role of surface silanol content in determining cellular toxicity [14]. Our results extend this concept to colloidal amorphous silica, which is generally considered less hemolytic than pyrogenic silica [42], thereby underscoring the significance of surface silanol groups in mediating particle–cell membrane interactions and cytotoxicity.

Characterization of SiO_2NPs: greater hydrodynamic diameter of OH-SIO_2NPs indicates stronger interaction with water or hydrophilic molecules in medium

SEM–EDX analysis revealed a greater abundance of nitrogen (N) and carbon (C) elements in NH_2-SiO_2NPs, likely derived from the NH_2 functional group and the diethylenetriamine linker on the particle surface. The higher silicon (Si) content observed in COOH-SiO_2NPs may originate from the (triethoxysilyl)propylsuccinic anhydride linker. These findings confirm the successful NH_2- and COOH-functionalization of the particles. Interestingly, the zeta potential of NH_2-SiO_2NPs was negative, although NH_2 groups are expected to be protonated under neutral or acidic conditions. According to the manufacturer's information, numerous acidic Si–OH groups remain on the surface of NH_2-SiO_2NPs, contributing to their overall negative zeta potential [43]. It is noteworthy that OH-SiO_2NPs exhibited a higher oxygen (O) content and a larger hydrodynamic diameter in both water and FBS-free medium compared with NH_2- or COOH-SiO_2NPs. These properties indicate stronger interactions of OH-SiO_2NPs with water or other hydrophilic molecules in the medium. In contrast, NH_2- and COOH-functionalization, through organic linkers, likely increases particle surface hydrophobicity, limiting their interaction with the medium and preventing an increase in hydrodynamic diameter.

OH-SiO_2NPs toxicity involves IL-1β and TNF-α upregulation

The higher expression levels of IL-1β and TNF-α after 1 h exposure to OH-SiO_2NPs or after 4 h exposure to OH-SiO_2NPs at non-cytotoxic level of 0.33 μg/cm^2 suggests the involvement of proinflammatory cytokines in the cytotoxicity of OH-SiO_2NPs.

Possible role of apoptotic/necroptotic pathways in OH-SiO_2NPs cytotoxicity

The use of each of inhibitors of apoptosis, necroptosis, pyroptosis and autophagy did not alter the cytotoxicity of OH-SiO2NPs. However, the combined use of apoptosis and necroptosis inhibitors reduced the cytotoxicity of OH-SiO_2NPs, suggesting the roles of these two pathways in OH- SiO_2NPs' cytotoxicity. In this regard, DAPI staining did not show nuclear fragmentation of RAW264.7 murine macrophages exposed to OH-SiO_2NPs s at 8.37 μg /cm^2 (28 μg/mL) for 18 h, suggesting non-apoptotic cell death (Suppl. Figure 5). As numerous studies have shown, necroptosis can occur when apoptotic signaling is inhibited, including in the absence of caspase-8 function [44–47]. Our results may therefore indicate that the necroptosis inhibitor was effective when necroptotic signaling was activated by caspase inhibition. Moreover, recent studies have revealed cross-talk between apoptosis, necroptosis, and pyroptosis, leading to the concept of a combined cell death pathway termed PANoptosis[48, 49]. Investigation of the possible involvement of PANoptosis, however, is beyond the scope of the present study.

Rationale for NP exposure level used in the study

With regard to the relation between the exposure levels by oropharyngeal aspiration used in our study to those achieved by inhalation, Osier et al. [50] found deposition of 690 μg of titanium dioxide in the lungs of male rats weighing 175 to 225 g (probably 9-week-old) after 2-h

exposure to ultrafine titanium dioxide at concentration of 125 mg/m^3. Since the alveolar surface areas of 9-week-old rats and 8-week-old mice are 4000 and 530 cm^2, respectively [51, 52], the estimated lung deposition of titanium dioxide in mice would be $690 \times 530/4000 = 91$ µg following exposure at 125 mg/m^3 for 2 h. Based on these estimations, the high dose of 200 µg used in our study is comparable to lung deposition after inhalation of ultrafine particles at concentration of 125 mg/m^3 for 4.4 h.

Limitations of the study

This study has several limitations. First, the presence of a fluorescent label may influence surface charge, accessibility of functional groups, or induce masking effects, potentially altering the interactions of the particles with biological systems. Second, the characterization of SiO_2NPs was limited. SEM–EDX confirmed increased nitrogen content in NH_2-SiO_2NPs, consistent with NH_2 functionalization, and increased silicon content in COOH-SiO_2NPs, consistent with the COOH linker. However, the absolute degree of functionalization was not quantified. Attempts to evaluate NH_2 and COOH functionalization using Fourier-transform infrared spectroscopy (FTIR) with both attenuated total reflection (ATR) and KBr pellet methods failed to detect sufficient signals corresponding to the surface functional groups. Third, a greater hydrodynamic diameter of OH-SiO_2NPs indicates stronger interactions with water or other hydrophilic molecules, investigation of the protein corona formed around the particles would be meaningful; however, this was not examined in the present study.

Conclusions

The results of the present study demonstrate that surface modification of OH–SiO_2NPs with amino or carboxyl functional groups attenuated the OH-SiO_2NP-induced increase in lung weight in mice and reduced cytotoxicity in murine macrophages. Our findings further suggest that OH-SiO_2NP-induced cytotoxicity is not mediated by nanoparticle internalization but rather by apoptotic and necroptotic signaling triggered upon interaction of the nanoparticles with the cell membrane. These results highlight the potential for developing safer silica nanomaterials through amino- or carboxyl functionalization of surface silanols.

Supplementary Information

The online version contains supplementary material available at https://doi.org/10.1186/s12989-025-00653-6.

Supplementary material 1.

Supplementary material 2.

Supplementary material 3. Table 1. Effect test for factors in multiple regression model for BALF cell count. Table 2. Effect test for factors in multiple regression model for number and percentage of BALF macrophages or neutrophils with internalize SiO_2NPs. Table 3. Effect test for factors in multiple regression model for MTS viability assay. Table 4. Effect test for factors in multiple regression model for gene expression. Fig. 1. Absorbance in MTS assay for three types of SiO_2NPs. ANOVA followed by Dunnet multiple comparison test was applied to test for differences among the three types of SiO_2NPs. Significant level was set at 5%. Fig. 2. LDH cytotoxicity of three types of SiO_2NPs by different duration of exposure. RAW264.1 cells were plated at 10^4 cells/well in 100 µl of medium onto a 96-well tissue culture plate. After incubation at 37 ºC and 5% CO_2 for 24 hours, the cells were exposed to bare, carboxyl functionalize, amino functionalized rhodamine labeled silica nanoparticles at 5.85 µg /cm^2 (19.5 µg/mL). The LDH activity in the supernatant of the culture medium was measured after 1, 4, 12, 24, 36 and 48 hours exposure to the silica nanoparticles. Fig. 3. Evaluation of OH-SiO_2NPs-induced interference in MTS assay. Possible interference by hydroxylated silica nanoparticles (OH-SiO_2NPs) in the MTS assay was evaluated. OH-SiO_2NPs were dispersed in fetal bovine serum (FBS)-free cell culture medium at final concentrations ranging from 0.3 to 30 µg/cm^2 and incubated for 60 min at 37 ºC in 5% CO_2 with one of the following: (1) phenol red-free cell culture medium; (2) phenol red-free medium mixed with CellTiter 96® AQueous One Solution Reagent at a 5:1 ratio; or (3) 5 mL of phenol red-free medium containing 1 mL of CellTiter 96® AQueous One Solution Reagent and 50 µL of Na_2SO_3. After incubation, absorbance was measured at 490 nm. No significant differences between the different doses were observed (ANOVA). Significance level was set at 5%. Fig. 4. Optimal concentration of trypan blue for quenching fluorescence on the cell surface. The concentration of trypan blue required to quench the fluorescence of rhodamine was determined by plotting trypan blue and rhodamine intensity in RAW264.7 cells exposed to OH-SiO_2NPs. Fig. 5. Representative flow cytometric chart from RAW264.8 macrophages exposed to COOH-SiO_2NPs. RAW264.7 cells were seeded onto 6-well plates at 2.37 x 10^4 cells/cm^2 in complete cell culture medium and incubated for 24 h before treatment. After treatment with 3.0 mL/well of SiO_2NPs at the indicated concentrations for 1 or 4 h in the dark, the medium was removed, cultures were thoroughly washed three times with PBS and treated with 0.1% trypan blue for 1 min to quench the fluorescence of rhodamine on the cell surface. The cells were washed with PBS, mixed with 500 µL of FACS buffer (PBS containing 0.5% FBS and 0.1% NaN_3) and harvested by cell scraper. Cell-associated fluorescence was detected using FACSCaliburTM and the results were analyzed with FlowJo software (BD, Franklin Lakes, NJ). Data are the mean fluorescence intensity (MFI) of rhodamine (excitation 488 nm, filter range 564-606 nm) from three different size fractions indicated by the forward scatter (FS). Supplementary Fig. 6. Relation of different types of SiO_2NPs and rhodamine fluorescence. The intensity of rhodamine fluorescence was measured at different concentrations of three types of SiO_2NPs using ARVOMx-fla system (485 nm/535 nm 1.0 s). Regression lines were obtained by forcing the intercept to zero using Excel 2016 (Microsoft, Redmond, WA).

Acknowledgements

The authors are grateful to Dr. Kunichi Miyazawa for his valuable advice regarding this study. The authors also thank Ms. Kotomi Toriumi, Ms. Haruka Yonekura, Ms. Satoko Arai and Ms. Yuko Uozumi for the excellent secretarial supports.

Author contributions

SV, SI, SB, LT and GI designed the study and interpreted the data. SV, EW, WW and SI conducted animal studies. EW, KY, KaMi, ST and YO conducted in vitro studies. CZ, TSa, AS, YH, AI, TW, KuMi, YT, KMa, TSu and RA contributed to acquisition of the data. SV, EW, SI and GI drafted and revised the manuscript. All authors read and approved the final manuscript.

Funding

This work was supported by Japan Society for the Promotion of Science (JSPS) International Fellowship for Research in Japan (Short-term Program) #PE13040, JSPS NEXT Program #LS056 and Japan Science and Technology Agency (JST) Strategic Japanese-EU Cooperative Program: Study on managing the potential health and environmental risks of engineered nanomaterials.

Availability of data and materials

All generated and analyzed data are included in this published article and its supplementary information material.

Declarations

Ethics approval

This study was conducted according to the Japanese law on the protection and control of animals and the Animal Experimental Guidelines of Tokyo University of Science. The experimental protocol was approved by the Animal Ethics Committee of Tokyo University of Science (approval number: Y14059).

Competing interests

The authors declare no competing interests.

Author details

[1]Department of Occupational and Environmental Health, Faculty of Pharmaceutical Sciences, Tokyo University of Science, 6-3-1 Niijuku, Tokyo 125-8585, Japan
[2]Nano-Cell Biology Lab, Division of Cell Matrix Biology & Regenerative Medicine, School of Biological Sciences, and Centre for Nanotechnology in Medicine, Faculty of Biology, Medicine and Health, The University of Manchester, Manchester, UK
[3]National Institute of Materials Science, Tsukuba, Japan
[4]Jichi Medical University School of Medicine, Shimotsuke, Japan
[5]Department of Occupational and Environmental Health, Nagoya University Graduate School of Medicine, Nagoya, Japan
[6]Department of Biochemistry and Molecular Biology, Faculty of Pharmaceutical Sciences, Tokyo University of Science, Tokyo, Japan
[7]Research Institute of Biomedical Sciences, Tokyo University of Science, Noda, Japan
[8]Université Paris Cité, CNRS, Unité de Biologie Fonctionnelle et Adaptative, 75013 Paris, France
[9]Institute of Occupational Medicine, Edinburgh, UK

Received: 31 March 2025 / Accepted: 25 November 2025
Published online: 19 December 2025

References

1. Napierska D, Thomassen LC, Lison D, Martens JA, Hoet PH. The nanosilica hazard: another variable entity. Part Fibre Toxicol. 2010;7(1):39.
2. Murugadoss S, Lison D, Godderis L, Van Den Brule S, Mast J, Brassinne F, et al. Toxicology of silica nanoparticles: an update. Arch Toxicol. 2017;91(9):2967–3010.
3. Hansen SF, Michelson ES, Kamper A, Borling P, Stuer-Lauridsen F, Baun A. Categorization framework to aid exposure assessment of nanomaterials in consumer products. Ecotoxicology. 2008;17(5):438–47.
4. Kempen PJ, Greasley S, Parker KA, Campbell JL, Chang HY, Jones JR, et al. Theranostic mesoporous silica nanoparticles biodegrade after pro-survival drug delivery and ultrasound/magnetic resonance imaging of stem cells. Theranostics. 2015;5(6):631–42.
5. Hnizdo E, Sullivan PA, Bang KM, Wagner G. Association between chronic obstructive pulmonary disease and employment by industry and occupation in the US population: a study of data from the third national health and nutrition examination survey. Am J Epidemiol. 2002;156(8):738–46.
6. Hnizdo E, Vallyathan V. Chronic obstructive pulmonary disease due to occupational exposure to silica dust: a review of epidemiological and pathological evidence. Occup Environ Med. 2003;60(4):237–43.
7. Ross MH, Murray J. Occupational respiratory disease in mining. Occup Med. 2004;54(5):304–10.
8. Yu Y, Duan J, Yu Y, Li Y, Liu X, Zhou X, et al. Silica nanoparticles induce autophagy and autophagic cell death in HepG2 cells triggered by reactive oxygen species. J Hazard Mater. 2014;270:176–86.
9. Fedeli C, Selvestrel F, Tavano R, Segat D, Mancin F, Papini E. Catastrophic inflammatory death of monocytes and macrophages by overtaking of a critical dose of endocytosed synthetic amorphous silica nanoparticles/serum protein complexes. Nanomedicine. 2013;8(7):1101–26.
10. Ahmad J, Ahamed M, Akhtar MJ, Alrokayan SA, Siddiqui MA, Musarrat J, et al. Apoptosis induction by silica nanoparticles mediated through reactive oxygen species in human liver cell line HepG2. Toxicol Appl Pharmacol. 2012;259(2):160–8.
11. Nemmar A, Yuvaraju P, Beegam S, Yasin J, Dhaheri RA, Fahim MA, et al. In vitro platelet aggregation and oxidative stress caused by amorphous silica nanoparticles. Int J Physiol Pathophysiol Pharmacol. 2015;7(1):27–33.
12. Maser E, Schulz M, Sauer UG, Wiemann M, Ma-Hock L, Wohlleben W, et al. In vitro and in vivo genotoxicity investigations of differently sized amorphous SiO2 nanomaterials. Mutat Res Genet Toxicol Environ Mutagen. 2015;794:57–74.
13. Dostert C, Petrilli V, Van Bruggen R, Steele C, Mossman BT, Tschopp J. Innate immune activation through Nalp3 inflammasome sensing of asbestos and silica. Science. 2008;320(5876):674–7.
14. Rubio L, Pyrgiotakis G, Beltran-Huarac J, Zhang Y, Gaurav J, Deloid G, et al. Safer-by-design flame-sprayed silicon dioxide nanoparticles: the role of silanol content on ROS generation, surface activity and cytotoxicity. Part Fibre Toxicol. 2019;16(1):40.
15. Kusaka T, Nakayama M, Nakamura K, Ishimiya M, Furusawa E, Ogasawara K. Effect of silica particle size on macrophage inflammatory responses. PLoS ONE. 2014;9(3):e92634.
16. Morris AS, Adamcakova-Dodd A, Lehman SE, Wongrakpanich A, Thorne PS, Larsen SC, et al. Amine modification of nonporous silica nanoparticles reduces inflammatory response following intratracheal instillation in murine lungs. Toxicol Lett. 2016;241:207–15.
17. Marzaioli V, Aguilar-Pimentel JA, Weichenmeier I, Luxenhofer G, Wiemann M, Landsiedel R, et al. Surface modifications of silica nanoparticles are crucial for their inert versus proinflammatory and immunomodulatory properties. Int J Nanomedicine. 2014;9:2815–32.
18. Brandenberger C, Rowley NL, Jackson-Humbles DN, Zhang Q, Bramble LA, Lewandowski RP, et al. Engineered silica nanoparticles act as adjuvants to enhance allergic airway disease in mice. Part Fibre Toxicol. 2013;10:26.
19. Han B, Guo J, Abrahaley T, Qin L, Wang L, Zheng Y, et al. Adverse effect of nano-silicon dioxide on lung function of rats with or without ovalbumin immunization. PLoS ONE. 2011;6(2):e17236.
20. Park HJ, Sohn JH, Kim YJ, Park YH, Han H, Park KH, et al. Acute exposure to silica nanoparticles aggravate airway inflammation: different effects according to surface characteristics. Exp Mol Med. 2015;47:e173.
21. Han H, Park YH, Park HJ, Lee K, Um K, Park JW, et al. Toxic and adjuvant effects of silica nanoparticles on ovalbumin-induced allergic airway inflammation in mice. Respir Res. 2016;17(1):60.
22. Bagwe RP, Hilliard LR, Tan W. Surface modification of silica nanoparticles to reduce aggregation and nonspecific binding. Langmuir. 2006;22(9):4357–62.
23. Marzaioli V, Gross CJ, Weichenmeier I, Schmidt-Weber CB, Gutermuth J, Gross O, et al. Specific surface modifications of silica nanoparticles diminish inflammasome activation and in vivo expression of selected inflammatory genes. Nanomaterials. 2017. https://doi.org/10.3390/nano7110355.
24. Lankoff A, Arabski M, Wegierek-Ciuk A, Kruszewski M, Lisowska H, Banasik-Nowak A, et al. Effect of surface modification of silica nanoparticles on toxicity and cellular uptake by human peripheral blood lymphocytes in vitro. Nanotoxicology. 2013;7(3):235–50.
25. Morishige T, Yoshioka Y, Inakura H, Tanabe A, Yao X, Narimatsu S, et al. The effect of surface modification of amorphous silica particles on NLRP3 inflammasome mediated IL-1beta production. ROS Product Endosomal Rupture Biomater. 2010;31(26):6833–42.
26. Wu W, Ichihara G, Hashimoto N, Hasegawa Y, Hayashi Y, Tada-Oikawa S, et al. Synergistic effect of bolus exposure to zinc oxide nanoparticles on bleomycin-induced secretion of pro-fibrotic cytokines without lasting fibrotic changes in murine lungs. Int J Mol Sci. 2014;16(1):660–76.
27. Fleming TJ, Fleming ML, Malek TR. Selective expression of Ly-6G on myeloid lineage cells in mouse bone marrow. RB6-8C5 mAb to granulocyte-differentiation antigen (Gr-1) detects members of the Ly-6 family. J Immunol. 1993;151(5):2399–408.
28. Hestdal K, Ruscetti FW, Ihle JN, Jacobsen SE, Dubois CM, Kopp WC, et al. Characterization and regulation of RB6-8C5 antigen expression on murine bone marrow cells. J Immunol. 1991;147(1):22–8.
29. Vranic S, Gosens I, Jacobsen NR, Jensen KA, Bokkers B, Kermanizadeh A, et al. Impact of serum as a dispersion agent for in vitro and in vivo toxicological assessments of TiO2 nanoparticles. Arch Toxicol. 2017;91(1):353–63.
30. Orts-gil G, Natte K, Drescher D, Bresch H, Mantion A, Kneipp J, et al. Characterisation of silica nanoparticles prior to in vitro studies: from primary particles to agglomerates. J Nanopart Res. 2011;13(4):1593–604.
31. Tada-Oikawa S, Eguchi M, Yasuda M, Izuoka K, Ikegami A, Vranic S, et al. Functionalized surface-charged SiO2 nanoparticles induce pro-inflammatory responses, but are not lethal to Caco-2 cells. Chem Res Toxicol. 2020;33(5):1226–36.
32. Hirsch C. NM interference in the MTS assay Version 1.1 2016 [cited 2025 Oct 06]. https://nanopartikel.info/data/methodik/VIGO/V_MTS_interference.pdf.

33. Qin CC, Liu YN, Hu Y, Yang Y, Chen Z. Macrophage inflammatory protein-2 as mediator of inflammation in acute liver injury. World J Gastroenterol. 2017;23(17):3043–52.
34. Balamayooran G, Batra S, Balamayooran T, Cai S, Jeyaseelan S. Monocyte chemoattractant protein 1 regulates pulmonary host defense via neutrophil recruitment during *Escherichia coli* infection. Infect Immun. 2011;79(7):2567–77.
35. Aman J, van der Heijden M, van Lingen A, Girbes AR, van Nieuw Amerongen GP, van Hinsbergh VW, et al. Plasma protein levels are markers of pulmonary vascular permeability and degree of lung injury in critically ill patients with or at risk for acute lung injury/acute respiratory distress syndrome. Crit Care Med. 2011;39(1):89–97.
36. Yu T, Malugin A, Ghandehari H. Impact of silica nanoparticle design on cellular toxicity and hemolytic activity. ACS Nano. 2011;5(7):5717–28.
37. Morishige T, Yoshioka Y, Inakura H, Tanabe A, Yao X, Tsunoda S, et al. Cytotoxicity of amorphous silica particles against macrophage-like THP-1 cells depends on particle-size and surface properties. Pharmazie. 2010;65(8):596–9.
38. Zhao J, Bu DY, Zhang N, Tian DN, Ma LY, Yang HF. Cytotoxicity of mesoporous silica modified by amino and carboxyl groups on vascular endothelial cells. Environ Toxicol. 2021;36(7):1422–33.
39. Ferenc M, Katir N, Milowska K, Bousmina M, Majoral JP, Bryszewska M, et al. Haemolytic activity and cellular toxicity of SBA-15-type silicas: elucidating the role of the mesostructure, surface functionality and linker length. J Mater Chem B. 2015;3(13):2714–24.
40. Spyrogianni A, Herrmann IK, Keevend K, Pratsinis SE, Wegner K. The silanol content and in vitro cytolytic activity of flame-made silica. J Colloid Interface Sci. 2017;507:95–106.
41. Pavan C, Santalucia R, Leinardi R, Fabbiani M, Yakoub Y, Uwambayinema F, et al. Nearly free surface silanols are the critical molecular moieties that initiate the toxicity of silica particles. Proc Natl Acad Sci U S A. 2020;117(45):27836–46.
42. Zhang H, Dunphy DR, Jiang X, Meng H, Sun B, Tarn D, et al. Processing pathway dependence of amorphous silica nanoparticle toxicity: colloidal vs pyrolytic. J Am Chem Soc. 2012;134(38):15790–804.
43. MICROMOD. FAQ 13. Why is the zeta potential of silicate particles with amino groups on the surface negative?. https://micromod.de/en/help-service/.
44. Dillon CP, Oberst A, Weinlich R, Janke LJ, Kang TB, Ben-Moshe T, et al. Survival function of the FADD-CASPASE-8-cFLIP(L) complex. Cell Rep. 2012;1(5):401–7.
45. Kaiser WJ, Upton JW, Long AB, Livingston-Rosanoff D, Daley-Bauer LP, Hakem R, et al. RIP3 mediates the embryonic lethality of caspase-8-deficient mice. Nature. 2011;471(7338):368–72.
46. O'Donnell MA, Perez-Jimenez E, Oberst A, Ng A, Massoumi R, Xavier R, et al. Caspase 8 inhibits programmed necrosis by processing CYLD. Nat Cell Biol. 2011;13(12):1437–42.
47. Oberst A, Dillon CP, Weinlich R, McCormick LL, Fitzgerald P, Pop C, et al. Catalytic activity of the caspase-8-FLIP(L) complex inhibits RIPK3-dependent necrosis. Nature. 2011;471(7338):363–7.
48. Malireddi RKS, Kesavardhana S, Kanneganti TD. ZBP1 and TAK1: master regulators of NLRP3 inflammasome/pyroptosis, apoptosis, and necroptosis (PAN-optosis). Front Cell Infect Microbiol. 2019;9:406.
49. Shi C, Cao P, Wang Y, Zhang Q, Zhang D, Wang Y, et al. PANoptosis: a cell death characterized by pyroptosis, apoptosis, and necroptosis. J Inflamm Res. 2023;16:1523–32.
50. Osier M, Baggs RB, Oberdorster G. Intratracheal instillation versus intratracheal inhalation: influence of cytokines on inflammatory response. Environ Health Perspect. 1997;105(Suppl 5):1265–71.
51. Bianco T, Centore R, Giannetti P, Scuri R. Compared kinetics of 2-(2,3-dihydro-5-acetoxy-4,6,7-trimethylbenzofuranyl) acetic acid (IRFI 016) and its active metabolite 2-(2,3-dihydro-5-hydroxy-4,6,7-trimethylbenzofuranyl) acetic acid (IRFI 005) in plasma and bronchial alveolar liquid in mice. Drugs Exp Clin Res. 1992;18(3):93–7.
52. Kawakami M, Paul JL, Thurlbeck WM. The effect of age on lung structure in male BALB/cNNia inbred mice. Am J Anat. 1984;170(1):1–21.

Publisher's Note